

000
001  **PIXELS LIE, CODE DOESN'T: THINKING WITH VI-
002
003
004
005
006
007
008
009
010
011
012
013
014
015
016
017
018
019
020
021
022
023
024
025
026
027
028
029
030
031
032
033
034
035
036
037
038
039
040
041
042
043
044
045
046
047
048
049
050
051
052
053** VISUAL PROGRAMMING FOR “SEEMINGLY IMPOSSIBLE”
004 MULTIMODAL AGENTIC REASONING TASKS

Anonymous authors

Paper under double-blind review

ABSTRACT

To overcome the inherent limitations of Chain-of-Thought (CoT) and to further push the upper bound of multimodal reasoning capabilities, we introduce Thinking with Visual Programming (TVP), where models can iteratively interact with an external code executor to generate, run, and verify both visual and textual agentic operations as part of the reasoning loop. Motivated by the open question of how far Multimodal Large Language Models (MLLMs) still lag behind this paradigm, we introduce **MMR-VIP**, a MultiModal Agentic Reasoning benchmark built on Visual Impossible Problems. We design MMR-VIP with two key principles: (1) We construct a **Difficulty Ladder** grounded in computational complexity theory, structuring tasks from easy problems that can be solved with inherent perception and reasoning, through medium problems that require external computational tools, to hard problems that remain intractable even with programming assistance. (2) We decompose the paradigm of Thinking with Visual Programming into three **Cognitive Skills**, namely **Perception**, **Abstraction**, and **Optimization**, which correspond to perceiving visual inputs, abstracting them into problem formulations, and optimizing algorithms to obtain efficient solutions. Our experiments on MMR-VIP yield the following findings: (1) GPT-5, as a native TVP model, delivers the strongest overall results, yet its accuracy remains only 38.2%, underscoring substantial room for progress. (2) For commercial models, multi-turn code execution consistently surpasses direct CoT and single-turn execution, providing stable and significant improvements. (3) Across difficulty levels, performance follows a ladder-shaped trend, with negligible gains on easy tasks, the largest improvements on medium tasks, and steady advances on hard tasks. (4) From a cognitive perspective, TVP enhances optimization by offloading complex computation, search, and planning, but models still encounter bottlenecks in abstraction.

1 INTRODUCTION

Multimodal reasoning is a defining capability of human intelligence, enabling us to address diverse challenges such as navigating in the physical world, interpreting scientific figures, and solving geometry problems (Yue et al., 2024; Lu et al., 2024). Recent advances in Multimodal Large Language Models (MLLMs) (OpenAI, 2024; DeepMind, 2025; Bai et al., 2025) have demonstrated significant progress by leveraging **Chain-of-Thought** (CoT) (Wei et al., 2022; Zhang et al., 2024c), which bridges perception and reasoning through explicit sequences of textual steps. Nevertheless, existing improvements remain constrained, since they primarily extend text-based CoT, prolonging the reasoning process without enhancing the upper bound of the model’s reasoning capabilities.

To address these limitations, “**Thinking with Images**” (TWI) (Zheng et al., 2025; Su et al., 2025a;c) has recently been proposed as an emerging paradigm, enabling models to incorporate iterative visual inspection as part of the reasoning loop. In practice, current methods rely on manipulating images with external tools (Zhang et al., 2025), such as cropping, zooming, rotating, and other image processing operations. Although such strategies enhance perceptual accuracy, they are limited to a narrow set of predefined visual tools, thereby rigidifying the reasoning process and restricting its generality. As various forms of visual manipulation can naturally be expressed and executed through programming, we propose the paradigm of “**Thinking with Visual Programming**” (TVP), which goes beyond fixed tools and allows models like OpenAI’s o4 and GPT-5 (OpenAI, 2025a) to flexibly generate, execute, and verify both visual and textual operations within the reasoning process.

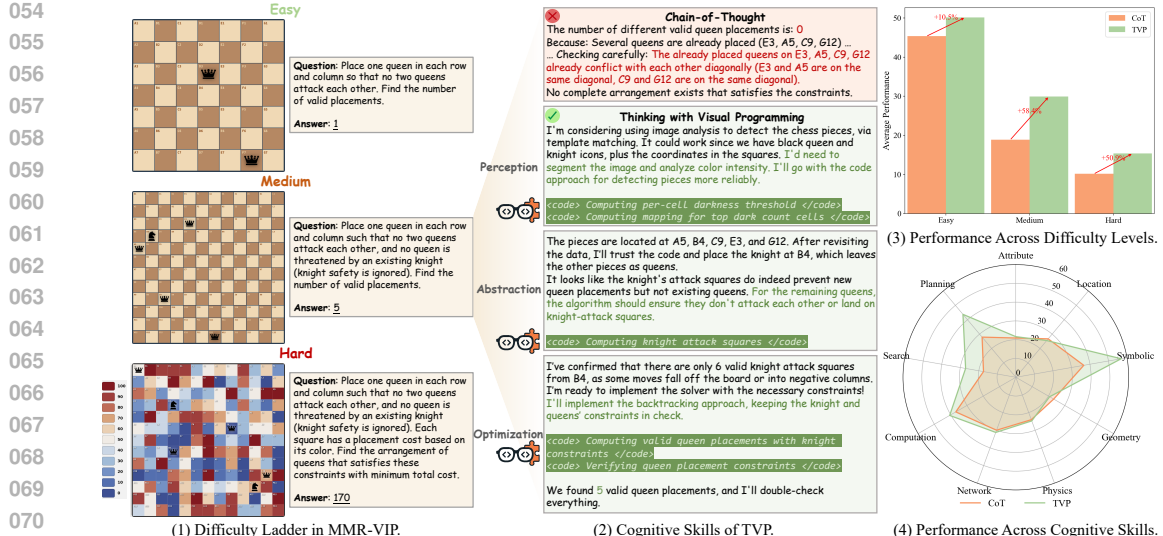


Figure 1: Thinking with Visual Programming paradigm. Figure 1(1) illustrates the three difficulty levels in MMR-VIP using the N-Queens task as an example. Figure 1(2) shows that for a medium-level problem, direct CoT reasoning fails while TVP succeeds, and in the process three key cognitive skills emerge. Figure 1(3) compares the average performance of four powerful models (GPT-4.1-mini, GPT-4.1, Gemini-2.5-Flash, and Claude-Sonnet-4) under CoT and TVP, showing minimal changes on easy tasks, the largest gains on medium tasks, and clear improvements on hard tasks. The results exhibit a ladder-shaped performance trend across difficulty levels. Figure 1(4) presents the performance differences of the four models across cognitive skills, where TVP yields notable improvements in symbolic (perception), computation, search, and planning (optimization).

Humans inherently solve complex reasoning problems in a programming-like manner by preprocessing visual inputs for better perception, applying algorithmic procedures to derive solutions, and verifying outcomes through testing. Nevertheless, it remains unclear how far current MLLMs are from this paradigm. To this end, we introduce **MMR-VIP**, a MultiModal Agentic Reasoning benchmark that consists of **Visual Impossible Problems**. Formally, we refer to Visual Impossible Problems as problems that appear intractable under CoT-based reasoning, yet become solvable when augmented with visual programming interactions. We design MMR-VIP with two key considerations:

Difficulty Ladder. We categorize problems into three levels of difficulty, drawing inspiration from how humans tackle tasks with and without tools, and grounded in computational complexity theory. (1) **Easy** level requires that the model can reliably solve them using its inherent perception and reasoning abilities, without any programming assistance. This level corresponds to “*low-complexity problems in P*”, where the model can perform reasoning within its working memory; (2) **Medium** level is challenging for the model to solve independently, but can be effectively addressed when it is allowed to use a code interpreter. This level typically involves “*polynomial-time solvable problems in P*”, where the model must rely on external computational tools to compute solutions; (3) **Hard** level remains unsolved even with programming assistance, often due to their large-scale computational complexity, highly intricate constraints, or demanding optimization requirements. This level corresponds conceptually to “*NP-hard problems*”, which often lie beyond the capabilities of current models. As shown in Figure 1(1), the three levels form a progressive difficulty ladder, where each step reflects an increasing demand on the model’s reasoning capacity and reliance on external tools.

Cognitive Skill. We decompose the Thinking with Visual Programming paradigm into three key cognitive skills, focusing on the core cognitive processes required to perceive, abstract, and optimize multimodal agentic reasoning. Taking the N-Queens problem in Figure 1(2) as an example: (1) **Perception** requires the model to transform *visual content* into *structured information*, correctly extracting relevant elements from multimodal inputs (e.g., detecting and locating chess pieces on the board); (2) **Abstraction** requires the model to transform *structured information* to *problem formulation*, producing computationally useful forms and proposing feasible solutions (e.g., converting piece positions into symbolic constraints that capture attack rules); (3) **Optimization** requires the model to transform *problem formulation* to *algorithmic optimization*, optimizing both algorithms

108 and computational procedures to obtain correct and efficient answers (e.g., applying a backtracking
 109 algorithm to search for valid queen placements under the given constraints).

110 MMR-VIP encompasses **28** carefully crafted task types, each designed across three difficulty levels,
 111 resulting in **1,680** instances that provide a comprehensive evaluation of multimodal agentic reason-
 112 ing capabilities. These tasks span a wide spectrum, from basic skills such as *counting* and *height*
 113 *measurement* to advanced challenges including *graph coloring* and *circuit logic*. To avoid dataset
 114 contamination and guarantee that models solve tasks via code execution instead of memorized recall,
 115 all problems in MMR-VIP are generated using carefully designed, manually written code.

116 We conduct a comprehensive evaluation on MMR-VIP across a wide range of MLLMs, including
 117 commercial models such as Claude-Sonnet-4, open-source models such as Qwen2.5-VL-72B, as
 118 well as native TVP models like o4-mini and GPT-5. We further assess different reasoning paradigms,
 119 including direct CoT, single-turn code execution, and multi-turn code execution. We obtain the fol-
 120 lowing conclusions: (1) Our experimental results reveal clear differences across model types and
 121 reasoning paradigms. For open-source models, introducing code execution provides little to no im-
 122 provement, mainly due to their limited visual programming capabilities. For commercial models,
 123 single-turn code execution yields unstable performance, while multi-turn code execution consis-
 124 tently delivers substantial gains. As illustrated in Figure 1(3), multi-turn code execution improves
 125 accuracy on medium-level tasks by **58.4%** compared to direct CoT. GPT-5, as a native TVP model,
 126 achieves the best overall performance; however, its accuracy remains only **38.2%**, indicating sub-
 127 stantial room for improvement; (2) Performances across different difficulty levels align well with the
 128 design of MMR-VIP, exhibiting a ladder-shaped performance trend. Compared to direct CoT, we
 129 observe that TVP yields minimal changes on easy tasks, the largest gains on medium tasks, and con-
 130 sistent improvements on hard tasks; (3) From the perspective of cognitive skills, TVP shows clear
 131 progress in optimization, as it can leverage programming to offload complex computation, search,
 132 and planning operations. However, its performance still encounters bottlenecks in abstraction, where
 133 models lack the ability to translate visual inputs into high-level problem formulations. We hope that
 134 MMR-VIP will serve as a challenging benchmark to drive future research toward closing this gap.

135 2 PARADIGM DEFINITIONS

136 2.1 MULTIMODAL CHAIN-OF-THOUGHT

139 We formalize the conventional paradigm of Multimodal Chain-of-Thought reasoning. For a model
 140 θ , given an input image I and a textual question x , the CoT process can be defined as:

$$141 \quad P_{\text{CoT}}(y | I, x) = P_{\theta}(r | I, x) \cdot P_{\theta}(y | I, x, r). \quad (1)$$

143 Here, $r = (s_1, s_2, \dots, s_n)$ denotes the intermediate reasoning chain, which explicitly captures the
 144 sequence of textual steps bridging perception and reasoning, while y represents the final answer
 145 conditioned on both the original input (I, x) and the generated textual rationale r .

146 2.2 THINKING WITH VISUAL PROGRAMMING

148 We formalize the proposed paradigm of Thinking with Visual Programming. For a model θ , given an
 149 input image I and textual question x , TVP extends conventional CoT by introducing programming
 150 actions a_t , which are executed through interaction with an external code executor \mathcal{E} . Unlike single-
 151 pass reasoning, this is a multi-turn interactive agentic process consisting of T rounds:

$$152 \quad P_{\text{TVP}}(y | I, x) = \prod_{t=1}^T P_{\theta}(r_t, a_t | s_{t-1}) \cdot P_{\theta}(y | s_T). \quad (2)$$

155 At each step t , the model generates a reasoning trace r_t and a programming action a_t , executes a_t
 156 via the external executor \mathcal{E} , and incorporates the multimodal execution result $\mathcal{E}(a_t)$ into the state s_t :

$$158 \quad s_t = s_{t-1} \cup \{r_t, a_t, \mathcal{E}(a_t)\}, \quad s_0 = \{I, x\}. \quad (3)$$

159 Compared to CoT, TVP offers significant advantages by integrating pixel manipulations and algo-
 160 rithmic computation into the reasoning loop, enabling models to move beyond textual thinking. In
 161 this paper, we do not provide models with fixed external tools. Instead, we allow them to write code
 that can call standard libraries, such as PIL, OpenCV, and Matplotlib, among others.

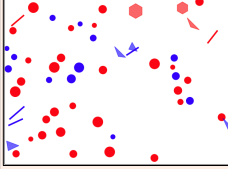
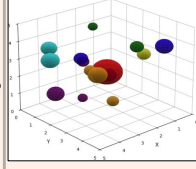
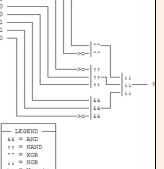
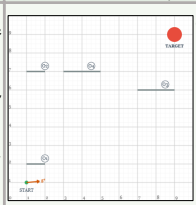
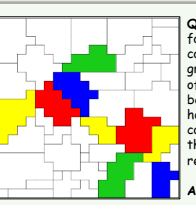
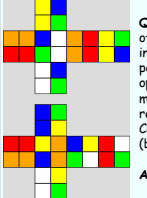
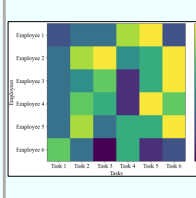
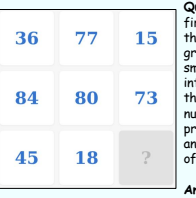
<p>(1) Attribute</p>  <p>Question: What is the number of red dots? Answer: 29</p>	<p>(2) Location</p>  <p>Question: What is the color of the ball at (2, 2, 2)? You can choose an answer from Red, Green, Orange, Cyan, Purple, Blue and Yellow. Answer: Red</p>	<p>(3) Symbolic</p>  <p>Question: This is a digital circuit problem. Given known input values for the circuit, determine the output value. Answer: 0</p>
<p>Difficulty: Hard Task: Point Counting</p>	<p>Difficulty: Medium Task: 3D Location</p>	<p>Difficulty: Easy Task: Circuit Logic</p>
<p>(4) Geometry</p>  <p>Question: Calculate the minimum enclosing rectangle area of the following rectangle, where the sides of the enclosing rectangle must be parallel to the grid. Answer: 63</p>	<p>(5) Physics</p>  <p>Question: How many ricochets will a ball launched from (1, 0) at 5° need to hit the target at (9, 9, 0)? The ball reflects perfectly off the arena walls and mirror-obstacles. Answer: 8</p>	<p>(6) Network</p>  <p>Question: Given the following four-coloring problem graph, where part of the region has been pre-colored, how many coloring combinations are there for the remaining region? Answer: 34560</p>
<p>Difficulty: Easy Task: Bounding Box</p>	<p>Difficulty: Medium Task: Ricochet Ball</p>	<p>Difficulty: Hard Task: Graph Coloring</p>
<p>(7) Search</p>  <p>Question: This is a diagram of a Rubik's Cube. Given an initial state (above), you can perform the standard 18 operations to find the minimum number of moves required to get the Rubik's Cube to the given state (below). Answer: 6</p>	<p>(8) Planning</p>  <p>Question: Each task can only be assigned to one person, and each person can only be assigned one task. Compute the maximum total profit. Answer: 500</p>	<p>(9) Computation</p>  <p>Question: Given the first 8 numbers in the nine-square grid, calculate the smallest positive integer such that the sum of this number plus all previous numbers is an integer multiple of 20. Answer: 12</p>
<p>Difficulty: Hard Task: Rubik's Cube</p>	<p>Difficulty: Medium Task: Resource Allocation</p>	<p>Difficulty: Easy Task: Calculation</p>

Figure 2: Evaluation framework of cognitive skills in MMR-VIP.

3 MMR-VIP BENCHMARK

To investigate how far current MLLMs are from the paradigm of TVP, we introduce **MMR-VIP**, a **MultiModal Agentic Reasoning** benchmark that consists of **Visual Impossible Problems**. These are carefully designed problems that existing MLLMs cannot reliably solve with conventional CoT reasoning alone, but instead necessitate interaction with an external code executor. We will detail the design principles behind MMR-VIP, including its difficulty ladder and cognitive skill dimensions, and describe the benchmark construction process along with dataset statistics.

3.1 DIFFICULTY LADDER

We categorize problems in MMR-VIP into a three-level **Difficulty Ladder**, drawing inspiration from how humans tackle tasks of varying complexity and their reliance on external tools. At the **Easy** level, tasks can be reliably solved using the model’s inherent perception and reasoning abilities, without the need for programming assistance. These correspond to “*low-complexity problems in P*”, where solutions can be derived directly within the model’s working memory. The **Medium** level encompasses tasks that models struggle to solve on their own but can successfully address when supported by external tools such as code interpreters. These tasks align with “*polynomial-time solvable problems in P*”, where deriving solutions requires programmatic operations and computational tools beyond intuition alone. Finally, the **Hard** level captures problems that remain unsolved even with programming assistance, typically due to large-scale computational complexity, intricate constraints, or challenging optimization requirements. Conceptually, these tasks are analogous to “*NP-hard problems*”, which often exceed the practical capabilities of current models. Such a difficulty ladder setting enables a more in-depth examination of the paradigm of TVP.¹

¹The tasks in MMR-VIP are not strictly designed or guaranteed to align with formal complexity-theoretic definitions, but rather follow the spirit of increasing computational and cognitive demands.

216
217 Table 1: Mapping between cognitive skills and task types in MMR-VIP.
218
219

220 Category	221 Tasks
222 Attribute	3D Position, Bin Packing, Graph Coloring, Hanoi Tower, Point Counting, Resource Allocation, Rubik’s Cube, Sliding Puzzle, Snake Game, Three-Views
223 Location	3D Position, Bounding Box, Height Measurement, Point Counting, Projectile Motion, Snake Game, Three-Views
224 Symbolic	Calculation, Chart, Circuit Logic, House Robber, Interval DP, N-Puzzle, Projectile Motion, Tableau LP
225 Geometry	Area Measurement, Bounding Box, Rubik’s Cube, Three-Views
226 Physics	Circuit Logic, Projectile Motion, Ricochet Ball
227 Network	Graph Coloring, Graph Isomorphism
Search	Bin Packing, Bubble Sort, Calculation, Graph Coloring, Maze, N-Puzzle, N-Queens, Path Counting, Rubik’s Cube, Sliding Puzzle, Snake Game
Planning	Chart, Hanoi Tower, House Robber, Interval DP, Lights Out, Resource Allocation, Tableau LP
Computation	Calculation, Path Counting

228
229
230 3.2 COGNITIVE SKILL
231

232 Beyond task difficulty, we design MMR-VIP to emphasize the underlying **Cognitive Skills** required
233 for multimodal agentic reasoning under the TVP paradigm. These skills highlight the essential pro-
234 cesses through which models must learn to leverage external tools to approach complex problems.
235 We define three successive skills within TVP: **Perception**, **Abstraction**, and **Optimization**, which
236 together examine a model’s visual programming ability from complementary dimensions.

237 **Perception:** This skill concerns the model’s ability to accurately extract structured information from
238 raw visual inputs. Unlike direct pattern recognition that relies solely on intrinsic visual perception,
239 TVP enables models to enhance perception through programmatic operations such as counting,
240 measuring, and localization. For example, as shown in Figure 2(1), when a task requires precise
241 object counting, models that rely only on intrinsic perception often fail due to overlapping shapes,
242 varying sizes, or background noise. In contrast, TVP enables the model to generate code that ana-
243 lyzes pixel-level cues such as color and boundary lines, allowing it to count objects more accurately.
244 We evaluate this skill across three dimensions: **Attribute** (*i.e.*, color, shape, size), **Location** (*i.e.*,
245 positions, distances, spatial relations), and **Symbolic** (*i.e.*, digits, letters, or graphical symbols).

246 **Abstraction:** This skill concerns the model’s ability to transform low-level structured information into
247 higher-level problem formulations. It requires not only recognizing surface patterns but also
248 capturing the underlying rules and constraints, and converting them into computationally useful
249 forms. For instance, as illustrated in Figure 2(6), the model must write code to abstract the puzzle
250 into a network structure, representing each piece as a node and encoding adjacency relations as
251 edges. This code-based abstraction allows the model to perform further search or optimization
252 over the graph. In MMR-VIP, we evaluate abstraction across three dimensions: **Geometry** (*i.e.*,
253 geometric formulations), **Physics** (*i.e.*, physical laws), and **Network** (*i.e.*, graph structures).

254 **Optimization:** This skill focuses on the model’s ability to transform problem formulations into
255 efficient algorithmic solutions. It requires not only identifying feasible solutions but also refining
256 them to satisfy the given conditions. For example, as illustrated in Figure 2(7), the Rubik’s Cube
257 task requires the model to minimize the number of moves from an initial state to a target state. TVP
258 enables the model to generate and execute code that systematically explores the space of valid cube
259 operations, pruning redundant paths and converging to the optimal sequence of moves. We evaluate
260 this skill across three dimensions: **Search** (*i.e.*, depth-first search, breadth-first search), **Planning**
261 (*i.e.*, dynamic programming, linear programming), and **Computation** (*i.e.*, numerical calculations).

262
263 3.3 BENCHMARK CONSTRUCTION
264

265 To ensure that tasks are both solvable in the TVP paradigm and suitable for difficulty control, we
266 adopt a Code2Task generation framework. We recruited five annotators with strong backgrounds in
267 programming competitions and instructed them to write code that specifies task rules and automatically
268 generates the corresponding images², problems, and answers. As task difficulty increased, an-
269 notators were required to design new rules and introduce greater computational complexity, thereby
enriching the reasoning challenges. To facilitate this process, annotators were permitted to utilize

²We implemented visualization through HTML and Matplotlib.

270 Table 2: Experimental results on MMR-VIP. The best performance in each column is highlighted
 271 in **bold**. Red denotes cases where TVP underperforms CoT, while Green denotes cases where it
 272 outperforms CoT, with darker shades indicating larger magnitude of change.

273 274 275 Model	276 Difficulty Level			277 Cognitive Skill									278 Overall	
	279 Easy	280 Mid	281 Hard	282 Att	283 Loc	284 Sym	285 Geo	286 Phy	287 Net	288 Com	289 Sea	290 Pla		
Open-source Models														
Keye-VL-1.5-8B	CoT	28.0	11.4	4.8	12.0	9.3	21.2	11.2	8.3	27.5	35.0	15.6	14.3	14.8
	T=1	9.1	3.2	2.5	4.2	3.8	5.2	3.8	4.4	12.5	6.7	4.2	3.8	4.9 (↓ 9.9)
Gemma-3-27B	CoT	16.2	5.5	5.0	7.8	6.0	11.9	2.5	10.0	16.7	17.5	10.2	6.0	8.9
	T=1	15.5	10.0	4.1	6.2	5.5	17.3	4.2	6.7	22.5	28.3	8.9	10.2	9.9 (↑ 1.0)
Qwen2.5-VL-7B	CoT	13.2	7.0	3.9	7.5	3.6	7.3	3.8	8.9	26.7	6.7	6.8	6.4	8.0
	T=1	7.3	5.5	1.6	2.5	2.9	7.5	2.1	2.2	17.5	21.7	5.3	1.7	4.8 (↓ 3.2)
Qwen2.5-VL-32B	CoT	24.3	10.9	6.4	13.7	12.6	17.3	8.3	10.0	25.0	29.2	14.7	8.6	13.9
	T=1	13.6	4.6	4.1	7.7	8.1	6.9	4.2	9.4	13.3	6.7	5.9	4.8	7.4 (↓ 6.5)
Qwen2.5-VL-72B	T=3	18.9	9.8	6.8	10.0	8.8	18.3	2.5	7.2	20.8	28.3	13.3	10.7	11.8 (↓ 2.1)
	CoT	23.9	10.4	6.1	12.3	10.7	15.8	12.5	8.9	30.8	20.8	12.1	8.6	13.4
Qwen2.5-VL-72B	T=1	20.5	9.6	4.5	11.5	11.7	16.2	5.8	7.8	18.3	15.8	9.1	10.9	11.6 (↓ 1.8)
Commercial Models														24.2
GPT-4.1-mini	CoT	42.7	20.2	9.8	23.3	23.8	32.1	19.6	21.1	30.8	34.2	18.9	26.9	29.3 (↑ 5.1)
	T=1	45.5	28.2	14.1	16.0	23.3	49.4	22.1	22.2	35.0	39.2	24.7	37.1	28.2 (↑ 4.0)
GPT-4.1	T=3	42.1	28.4	14.1	21.8	21.4	45.0	16.2	14.4	31.7	31.7	22.9	40.5	24.3
	CoT	42.7	19.1	11.1	23.0	26.9	33.8	20.0	26.1	30.0	35.0	13.9	28.6	28.3 (↓ 2.9)
Gemini-2.5-Flash	T=1	38.9	18.0	7.1	18.7	23.8	25.4	22.1	27.2	27.5	22.5	17.6	16.4	21.4 (↓ 6.8)
	T=3	47.1	25.5	12.1	18.7	25.0	50.4	13.8	32.8	28.3	32.5	20.3	36.9	28.3 (↑ 4.0)
Gemini-2.5-Flash	CoT	46.4	18.0	10.9	17.8	27.6	42.5	26.2	25.6	32.5	40.0	17.7	28.1	25.1
	T=1	32.7	14.5	7.9	9.0	17.4	34.2	22.1	25.0	12.5	32.5	14.4	19.5	18.3 (↓ 6.8)
Gemini-2.5-Pro	T=3	59.3	34.5	16.1	21.8	30.2	64.6	27.1	33.3	29.2	40.0	30.0	49.0	36.6 (↑ 11.5)
	CoT	58.0	20.9	10.4	21.3	25.7	44.4	29.6	29.4	27.5	37.5	26.2	32.9	29.8
Claude-Sonnet-4	T=1	38.8	20.2	11.4	12.7	17.9	38.3	20.0	30.0	27.5	16.7	16.5	29.5	23.4 (↓ 6.4)
	CoT	49.6	18.2	8.9	19.5	28.6	38.3	27.1	23.3	26.7	38.3	19.2	28.1	25.6
Claude-Sonnet-4	T=1	49.5	31.6	14.3	22.0	27.6	53.5	19.6	26.1	28.3	45.8	28.6	38.3	31.8 (↑ 6.2)
Native TVP Models														35.2
o4-mini		57.7	30.7	17.3	28.0	24.8	55.4	25.4	26.1	35.0	40.0	27.3	55.2	36.1
	GPT-5-mini		61.8	29.8	16.8	32.7	29.8	52.9	27.9	26.1	32.5	42.5	28.3	53.3
GPT-5		65.5	33.8	15.4	27.5	31.7	60.4	30.8	31.1	39.2	39.2	28.2	56.9	38.2
Reference														36.1
Human		69.6	55.4	35.7	48.3	54.8	75.0	37.5	27.8	58.3	66.7	50.0	69.1	53.6

300 AI-assisted code editors (*e.g.*, Cursor). Finally, we conducted cross-validation of all generated code
 301 to verify correctness, where each program was independently reviewed by multiple annotators.

302 In total, MMR-VIP encompasses **28** carefully crafted task types, each designed across three dif-
 303 ficulty levels. For every task and difficulty, we randomly generated **20** instances, resulting in a
 304 benchmark of **1,680** instances in total. We include detailed examples of each task in the Appendix
 305 **C**. The mapping between task types and their corresponding cognitive skills is presented in Table 1.
 306 Since all tasks are synthesized from code, MMR-VIP is reproducible and extendable. Researchers
 307 can regenerate new instances by adjusting parameters or extend the benchmark with new task rules,
 308 making MMR-VIP a continuously evolvable framework rather than a fixed dataset.

310 4 EXPERIMENTS

311 In this section, we present a comprehensive evaluation of existing MLLMs on MMR-VIP. We sys-
 312 tematically evaluate model performance across different difficulty levels and cognitive skills, and
 313 further contrast the effectiveness of CoT and TVP. We also analyze from multiple perspectives, in-
 314 cluding the effect of iteration rounds, the role of input modalities, and the distribution of error types.

315 4.1 EXPERIMENTAL SETUP

316 We evaluate three categories of MLLMs on MMR-VIP: commercial models (*e.g.*, GPT-4.1 ([Ope-](#)
 317 [nAI, 2025b](#)), Gemini-2.5-Flash, Gemini-2.5-Pro ([DeepMind, 2025](#)), Claude-Sonnet-4 ([Anthropic,](#)
 318 [2025](#))), open-source models (*e.g.*, Qwen2.5-VL ([Bai et al., 2025](#)), Gemma-3 ([Kamath et al., 2025](#)),
 319 Keye-VL-1.5 ([Yang et al., 2025a](#))), and native TVP models (*e.g.*, o4-mini, GPT-5). We do not
 320 include existing open-source models designed specifically for Thinking with Images, since these
 321 models primarily focus on applying fixed transformations to images rather than freely generating
 322 models.

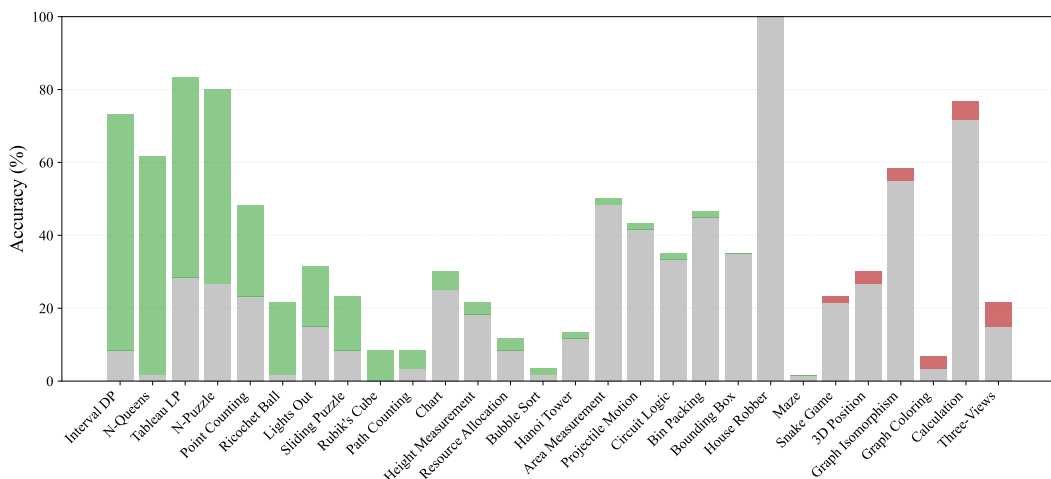


Figure 3: Performance comparison of Gemini-2.5-Flash on different tasks under CoT and TVP ($T = 3$). Gray indicates the baseline performance of CoT, Green indicates improvements of TVP over CoT, and Red indicates degradations of TVP over CoT.

code to support reasoning. Moreover, to assess the effectiveness of different reasoning strategies, we compare three settings: **Chain-of-Thought**, **single-turn TVP**, where the model invokes the code executor once, and **multi-turn TVP**, where the model can iteratively generate, execute, and refine code for up to $T = 3, 5, 7$ rounds. We provide the detailed prompts used for all settings in the Appendix D. As a reference, we randomly sample 168 instances and invite human participants to solve these tasks. Each participant is allowed to leverage search engines and interpreters during the process. We adopt accuracy as the evaluation metric. We report results along three perspectives: performance across different difficulty levels, performance across distinct cognitive skills, and the overall accuracy.

4.2 EXPERIMENTAL RESULTS

As shown in the Table 2, our experiments on MMR-VIP yield several key findings:

(1) **Performance differences across model types and reasoning paradigms.** For open-source models like Qwen2.5-VL-72B, introducing TVP offers negligible gains and sometimes results in performance drops, owing to their limited visual programming capabilities. For commercial models, single-turn code execution produces unstable results, whereas multi-turn execution consistently yields significant improvements. For instance, Gemini-2.5-Flash shows an accuracy gain of 18.3% when increasing from $T = 1$ to $T = 3$. For native TVP models, although GPT-5 achieves the highest performance, it attains only **38.2%** accuracy, reflecting the substantial limitations that remain. We can observe a clear performance gap relative to humans, underscoring that humans are more adept at leveraging external tools to solve complex visual problems.

(2) **Clear difficulty ladder.** The results align closely with the benchmark’s design, showing a distinct ladder-shaped performance trend. Compared to direct CoT, TVP shows negligible differences on easy tasks, achieves the largest improvements on medium tasks, and delivers consistent gains on hard tasks. Nevertheless, performance at the hard level remains very low, with the best accuracy reaching only 17.3%. This demonstrates that MMR-VIP effectively stratifies problems by difficulty, thereby exposing the limits of current MLLMs’ reasoning capabilities.

(3) **Imbalanced cognitive skills.** The results reveal marked disparities across cognitive skills. TVP delivers the most significant improvements in Optimization, where models effectively leverage programmatic search, planning, and computation to tackle complex problem-solving tasks. As shown in Figure 3, Gemini-2.5-Flash exhibits large gains on tasks such as *Interval Dynamic Programming*, *N-Queens*, *Tableau Linear Programming*, and *N-Puzzle*, where code execution is essential to explore solution spaces. In addition, TVP also enhances Symbolic perception, since code allows models to precisely recognize, parse, and manipulate digits, letters, or graphical symbols. However, performance in Abstraction remains the most challenging, where models still struggle to translate

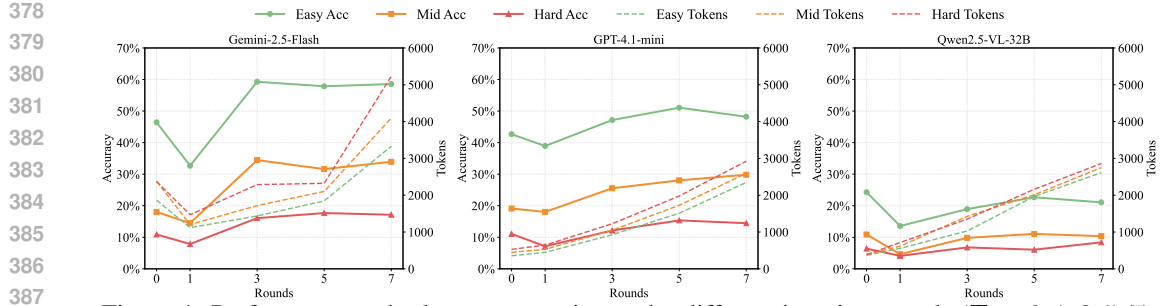


Figure 4: Performance and token consumption under different iteration rounds ($T = 0, 1, 3, 5, 7$). $T = 0$ corresponds to CoT. Green, orange, and red correspond to Easy, Medium, and Hard levels.

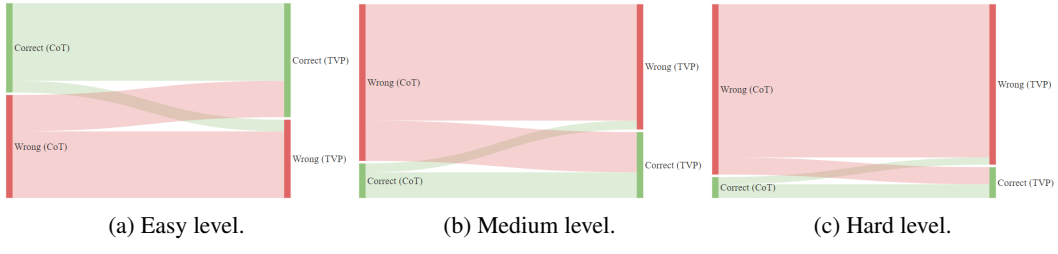


Figure 5: Correctness flow between CoT ($T = 0$) and TVP ($T = 3$) for Gemini-2.5-Flash.

low-level visual cues into high-level formulations such as geometric equations, physical laws, or graph structures. This underscores the necessity of improving their ability to abstract through code.

4.3 ANALYSIS

4.3.1 IMPACT OF ITERATION ROUNDS

We examine the impact of iterative rounds of code execution on model performance across easy, medium, and hard tasks. As shown in Figure 4, compared to direct CoT, single-turn TVP ($T = 1$) often leads to a drop in accuracy. To better understand this phenomenon, we compute the correlation between the performance difference of TVP ($T = 1$) versus CoT and the success rate of program execution. The Pearson correlation coefficient is **0.81** ($p \approx 0.05$), indicating a strong positive relationship. A primary source of degradation arises when incorrect code execution propagates interpreter error messages into the reasoning process, thereby misguiding subsequent inference.

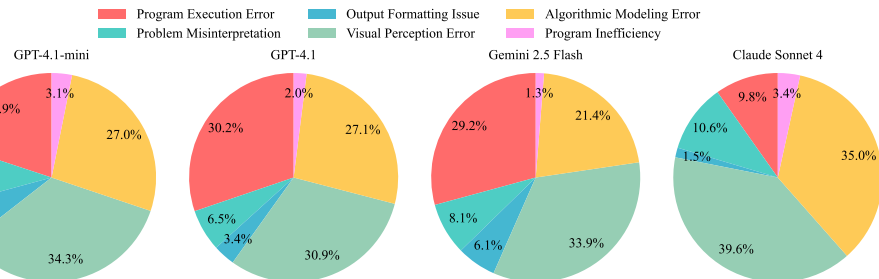
Performance generally peaks at $T = 3$ or $T = 5$, where iterative refinement enables more reliable program execution and reflective reasoning. As illustrated in Figure 5, we further analyze the correctness flow between CoT and TVP ($T = 3$). The results show that the most significant changes occur at the Medium difficulty level. However, for open-source models like Qwen2.5-VL-32B, additional iterations fail to bring noticeable gains. This finding highlights that robust visual programming capabilities are indispensable for open-source models to fully realize the benefits of TVP. Meanwhile, increasing to $T = 7$ brings little to no additional gains and instead results in significantly higher token consumption, highlighting the trade-off between accuracy and efficiency.

4.3.2 INFLUENCE OF INPUT MODALITIES

To further investigate the role of input modalities in TVP, we select four tasks from MMR-VIP that can be represented in both textual and visual forms: *Tableau LP*, *Chart*, *Graph Coloring*, and *Maze*. This design allows us to directly compare model performance under three conditions: (1) image-only input (I), (2) text-only input (T), and (3) combined image-text input (I & T). Results in Table 3 show that text input generally outperforms image input, indicating that current models still have weaker visual reasoning capabilities. Moreover, visual inputs sometimes introduce perception errors, which can

Table 3: Performance comparison under different input modalities.

Model	I	T	I & T
GPT-4.1-mini	26.3	75.0	76.3
Claude-Sonnet-4	7.5	50.0	63.8
GPT-5-mini	5.0	50.0	53.8
GPT-5	25.0	46.3	70.0

Figure 6: Error analysis of four models under TVP ($T = 1$).

propagate through subsequent reasoning steps. Nevertheless, combined multimodal input consistently surpasses unimodal input, particularly on tasks where the visual layout conveys structural or spatial constraints that are difficult to capture with text alone.

4.3.3 ERROR ANALYSIS

To better understand the limitations of TVP, we conduct a detailed error analysis by categorizing incorrect predictions into six major types: Program Execution Error, Visual Perception Error, Algorithmic Modeling Error, Program Inefficiency, Problem Misinterpretation, and Output Formatting Issue. The precise definitions and representative examples of each category are provided in the Appendix F. As illustrated in Figure 6, the most common sources of error are Visual Perception Error, Algorithmic Modeling Error, and Program Execution Error. These results align with our earlier findings: they reflect (1) the insufficiency of models in Perception and Abstraction, where they struggle to accurately extract information from visual inputs and transform it into computationally useful formulations, and (2) the limitations of current models’ programming capabilities, where code errors remain prevalent. We also provide several case studies of CoT and TVP in Appendix G.

5 RELATED WORKS

Multimodal Reasoning. Multimodal reasoning has recently become a prominent frontier in AI research, with an expanding set of benchmarks and investigations underscoring its pivotal importance across domains such as interpreting scientific diagrams (Yue et al., 2024; Guo et al., 2025), solving geometry problems (Zhang et al., 2024b; Wang et al., 2024), and tackling visual puzzles (Chia et al., 2024; Ghosal et al., 2025; Song et al., 2025). Recent work (Huang et al., 2025; Meng et al., 2025; Chris et al., 2025; Hong et al., 2025; Deng et al., 2025; Wang et al., 2025c;b) has focused on enhancing models’ reasoning ability through reinforcement learning, thereby extending reasoning depth, enabling reflection and verification, and improving performance on complex tasks. However, some studies argue that RL is constrained by an invisible leash (Wu et al., 2025a), preventing it from discovering new reasoning trajectories beyond the model’s initial capabilities (Lin & Xu, 2025).

Visual Programming. Visual programming (Yang et al., 2025b; Surís et al., 2023; Hu et al., 2024b) requires models to generate executable code based on visual inputs. MMCode (Li et al., 2024) evaluates MLLMs’ code generation abilities on competitive-programming problems presented with visual contexts. HumanEval-V (Zhang et al., 2024a) is a benchmark designed to evaluate complex diagram understanding and visual reasoning abilities in programming contexts. It assesses whether models can accurately infer the underlying rules embedded in visual diagrams and subsequently generate correct programs that satisfy the corresponding test cases. Moreover, SWE-bench Multimodal (Yang et al., 2025b) evaluates agents on their ability to fix bugs in visual, user-facing JavaScript software, with tasks that incorporate images within their problem statements or test cases. Built upon the Mini-level of the XLogoOnline platform, XLogoOnline-Mini (Wen et al., 2025) requires models to synthesize programs that control a turtle navigating through a grid to accomplish a specified goal. The benchmark evaluates a broad spectrum of capabilities, including mathematical reasoning, logical reasoning, spatial understanding, and planning. The primary difference of our work, MMR-VIP, is that it aims to evaluate a model’s multimodal reasoning capabilities, where code serves only as an optional tool to enhance reasoning rather than being the final output. All code generated in MMR-VIP is free-form and intended solely to assist in problem-solving.

486 **Tool-Integrated Reasoning.** Rather than relying solely on parametric knowledge within the model,
 487 tool-integrated reasoning (TIR) (Jin et al., 2025; Li et al., 2025; Xue et al., 2025; Feng et al., 2025;
 488 Dong et al., 2025) enables the model to reason with external tools, such as a Python interpreter. Ex-
 489 tending this idea to multimodal settings, the paradigm of Thinking with Images (TWI) has emerged
 490 as an effective approach (Lu et al., 2025; Su et al., 2025b;a; Lai et al., 2025; Wang et al., 2025d; Wu
 491 et al., 2025b; Zhou et al., 2025). Instead of relying solely on textual reasoning, models are equipped
 492 with a predefined set of visual tools such as cropping, zooming, or rotating, which allow them to
 493 refine perception during problem solving. Recently, there has been a growing trend of enabling
 494 MLLMs to generate executable code as part of the reasoning process (Tang et al., 2025; Zhao et al.,
 495 2025; Hu et al., 2024a; Zhang et al., 2025; Wang et al., 2025a), showcasing the potential of the TVP.
 496

497 6 CONCLUSION

498 In this work, we introduced MMR-VIP, a benchmark designed to evaluate multimodal agentic rea-
 499 soning under the Thinking with Visual Programming paradigm. Beyond text-based CoT and fixed
 500 visual tools, TVP allows models to flexibly generate, execute, and refine programmatic code, which
 501 serve as intermediate reasoning steps to facilitate multimodal problem solving. MMR-VIP is specif-
 502 ically crafted for this paradigm, featuring problems that are unsolvable under CoT-based reasoning
 503 but become tractable when integrated with visual programming interactions. Progress in multimodal
 504 agentic reasoning will depend critically on strengthening models’ coding proficiency, enhancing
 505 their visual abstraction ability, and equipping them with multi-round iterative reasoning strategies.
 506

507
 508
 509
 510
 511
 512
 513
 514
 515
 516
 517
 518
 519
 520
 521
 522
 523
 524
 525
 526
 527
 528
 529
 530
 531
 532
 533
 534
 535
 536
 537
 538
 539

540 ETHICS STATEMENT
541

542 All experimental procedures involving human participants were conducted in accordance with the
543 relevant ethical guidelines. Moreover, all data instances in our benchmark are puzzle-style prob-
544 lems that are automatically synthesized through scripts rather than collected from real-world human
545 data. As such, the dataset contains no personal, harmful, or biased information. This ensures that
546 MMR-VIP is entirely safe for research and avoids introducing any sensitive or ethically problematic
547 content.

548
549 REPRODUCIBILITY STATEMENT
550

551 Our dataset is entirely script-synthesized rather than manually annotated or generated by LLMs, en-
552 suring full reproducibility. To facilitate this, we will release the synthesis scripts with fixed random
553 seeds alongside the final MMR-VIP dataset. We also provide data examples in the supplementary
554 materials. In addition, we provide detailed prompts used in all experiments in Appendix D, and
555 we will open-source the evaluation code together with the Python interpreter environment. This
556 guarantees that researchers can faithfully reproduce our experimental results.

557
558 REFERENCES
559

560 Anthropic. Introducing claude 4, May 2025. URL <https://www.anthropic.com/news/claude-4>.

562 Shuai Bai, Keqin Chen, Xuejing Liu, Jialin Wang, Wenbin Ge, Sibo Song, Kai Dang, Peng Wang,
563 Shijie Wang, Jun Tang, Humen Zhong, Yuanzhi Zhu, Ming-Hsuan Yang, Zhaohai Li, Jianqiang
564 Wan, Pengfei Wang, Wei Ding, Zheren Fu, Yiheng Xu, Jiabo Ye, Xi Zhang, Tianbao Xie, Zesen
565 Cheng, Hang Zhang, Zhibo Yang, Haiyang Xu, and Junyang Lin. Qwen2.5-vl technical report.
566 *CoRR*, abs/2502.13923, 2025. doi: 10.48550/ARXIV.2502.13923. URL <https://doi.org/10.48550/arXiv.2502.13923>.

568 Yew Ken Chia, Vernon Toh, Deepanway Ghosal, Lidong Bing, and Soujanya Poria. Puz-
569 zlevqa: Diagnosing multimodal reasoning challenges of language models with abstract vi-
570 sual patterns. In Lun-Wei Ku, Andre Martins, and Vivek Srikumar (eds.), *Findings of the*
571 *Association for Computational Linguistics, ACL 2024, Bangkok, Thailand and virtual meet-*
572 *ing, August 11-16, 2024*, pp. 16259–16273. Association for Computational Linguistics, 2024.
573 doi: 10.18653/V1/2024.FINDINGS-ACL.962. URL <https://doi.org/10.18653/v1/2024.findings-acl.962>.

575 Chris, Yichen Wei, Yi Peng, Xiaokun Wang, Weijie Qiu, Wei Shen, Tianyidan Xie, Jiangbo Pei,
576 Jianhao Zhang, Yunzhuo Hao, Xuchen Song, Yang Liu, and Yahui Zhou. Skywork R1V2: multi-
577 modal hybrid reinforcement learning for reasoning. *CoRR*, abs/2504.16656, 2025. doi: 10.48550/
578 ARXIV.2504.16656. URL <https://doi.org/10.48550/arXiv.2504.16656>.

580 Google DeepMind. Gemini flash, 2025. URL <https://deepmind.google/technologies/gemini/flash/>.

582 Yihe Deng, Hritik Bansal, Fan Yin, Nanyun Peng, Wei Wang, and Kai-Wei Chang. Openvlthinker:
583 An early exploration to complex vision-language reasoning via iterative self-improvement. *CoRR*,
584 abs/2503.17352, 2025. doi: 10.48550/ARXIV.2503.17352. URL <https://doi.org/10.48550/arXiv.2503.17352>.

586 Guanting Dong, Hangyu Mao, Kai Ma, Licheng Bao, Yifei Chen, Zhongyuan Wang, Zhongxia
587 Chen, Jiazen Du, Huiyang Wang, Fuzheng Zhang, Guorui Zhou, Yutao Zhu, Ji-Rong Wen, and
588 Zhicheng Dou. Agentic reinforced policy optimization. *CoRR*, abs/2507.19849, 2025. doi: 10.
589 48550/ARXIV.2507.19849. URL <https://doi.org/10.48550/arXiv.2507.19849>.

591 Jiazhan Feng, Shijue Huang, Xingwei Qu, Ge Zhang, Yujia Qin, Baoquan Zhong, Chengquan Jiang,
592 Jinxin Chi, and Wanjun Zhong. Retool: Reinforcement learning for strategic tool use in llms.
593 *CoRR*, abs/2504.11536, 2025. doi: 10.48550/ARXIV.2504.11536. URL <https://doi.org/10.48550/arXiv.2504.11536>.

594 Deepanway Ghosal, Vernon Toh, Yew Ken Chia, and Soujanya Poria. Algopuzzlevqa: Diagnos-
 595 ing multimodal reasoning challenges of language models with algorithmic multimodal puzzles.
 596 In Luis Chiruzzo, Alan Ritter, and Lu Wang (eds.), *Proceedings of the 2025 Conference of the*
 597 *Nations of the Americas Chapter of the Association for Computational Linguistics: Human Lan-*
 598 *guage Technologies, NAACL 2025 - Volume 1: Long Papers, Albuquerque, New Mexico, USA,*
 599 *April 29 - May 4, 2025*, pp. 9615–9632. Association for Computational Linguistics, 2025. doi:
 600 10.18653/V1/2025.NAACL-LONG.486. URL <https://doi.org/10.18653/v1/2025.nacl-long.486>.

602 Ziyu Guo, Renrui Zhang, Hao Chen, Jialin Gao, Dongzhi Jiang, Jiaze Wang, and Pheng-Ann Heng.
 603 Sciverse: Unveiling the knowledge comprehension and visual reasoning of lmms on multi-modal
 604 scientific problems. In Wanxiang Che, Joyce Nabende, Ekaterina Shutova, and Mohammad Taher
 605 Pilehvar (eds.), *Findings of the Association for Computational Linguistics, ACL 2025, Vienna,*
 606 *Austria, July 27 - August 1, 2025*, pp. 19683–19704. Association for Computational Linguistics,
 607 2025. URL <https://aclanthology.org/2025.findings-acl.1010/>.

608 Wenyi Hong, Wenmeng Yu, Xiaotao Gu, Guo Wang, Guobing Gan, Haomiao Tang, Jiale Cheng,
 609 Ji Qi, Junhui Ji, Lihang Pan, Shuaiqi Duan, Weihan Wang, Yan Wang, Yean Cheng, Zehai He,
 610 Zhe Su, Zhen Yang, Ziyang Pan, Aohan Zeng, Baoxu Wang, Boyan Shi, Changyu Pang, Chenhui
 611 Zhang, Da Yin, Fan Yang, Guoqing Chen, Jiazheng Xu, Jiali Chen, Jing Chen, Jinhao Chen,
 612 Jinghao Lin, Jinjiang Wang, Junjie Chen, Leqi Lei, Letian Gong, Leyi Pan, Mingzhi Zhang,
 613 Qinkai Zheng, Sheng Yang, Shi Zhong, Shiyu Huang, Shuyuan Zhao, Siyan Xue, Shangqin Tu,
 614 Shengbiao Meng, Tianshu Zhang, Tianwei Luo, Tianxiang Hao, Wenkai Li, Wei Jia, Xin Lyu,
 615 Xuancheng Huang, Yanling Wang, Yadong Xue, Yanfeng Wang, Yifan An, Yifan Du, Yiming
 616 Shi, Yiheng Huang, Yilin Niu, Yuan Wang, Yuanchang Yue, Yuchen Li, Yutao Zhang, Yuxuan
 617 Zhang, Zhanxiao Du, Zhenyu Hou, Zhao Xue, Zhengxiao Du, Zihan Wang, Peng Zhang, Debing
 618 Liu, Bin Xu, Juanzi Li, Minlie Huang, Yuxiao Dong, and Jie Tang. Glm-4.1v-thinking: Towards
 619 versatile multimodal reasoning with scalable reinforcement learning. *CoRR*, abs/2507.01006,
 620 2025. doi: 10.48550/ARXIV.2507.01006. URL <https://doi.org/10.48550/arXiv.2507.01006>.

622 Yushi Hu, Weijia Shi, Xingyu Fu, Dan Roth, Mari Ostendorf, Luke Zettlemoyer, Noah A.
 623 Smith, and Ranjay Krishna. Visual sketchpad: Sketching as a visual chain of thought
 624 for multimodal language models. In Amir Globersons, Lester Mackey, Danielle Bel-
 625 grave, Angela Fan, Ulrich Paquet, Jakub M. Tomczak, and Cheng Zhang (eds.), *Advances*
 626 *in Neural Information Processing Systems 38: Annual Conference on Neural Infor-*
 627 *mation Processing Systems 2024, NeurIPS 2024, Vancouver, BC, Canada, December 10 - 15,*
 628 *2024*, 2024a. URL http://papers.nips.cc/paper_files/paper/2024/hash/fb82011040977c7712409fbdb5456647-Abstract-Conference.html.

630 Yushi Hu, Otilia Stretcu, Chun-Ta Lu, Krishnamurthy Viswanathan, Kenji Hata, Enming Luo, Ran-
 631 jay Krishna, and Ariel Fuxman. Visual program distillation: Distilling tools and programmatic
 632 reasoning into vision-language models. In *IEEE/CVF Conference on Computer Vision and Pat-*
 633 *tern Recognition, CVPR 2024, Seattle, WA, USA, June 16-22, 2024*, pp. 9590–9601. IEEE, 2024b.
 634 doi: 10.1109/CVPR52733.2024.00916. URL <https://doi.org/10.1109/CVPR52733.2024.00916>.

636 Wenxuan Huang, Bohan Jia, Zijie Zhai, Shaosheng Cao, Zheyu Ye, Fei Zhao, Zhe Xu, Yao Hu, and
 637 Shaohui Lin. Vision-r1: Incentivizing reasoning capability in multimodal large language models.
 638 *CoRR*, abs/2503.06749, 2025. doi: 10.48550/ARXIV.2503.06749. URL <https://doi.org/10.48550/arXiv.2503.06749>.

640 Bowen Jin, Hansi Zeng, Zhenrui Yue, Dong Wang, Hamed Zamani, and Jiawei Han. Search-
 641 r1: Training llms to reason and leverage search engines with reinforcement learning. *CoRR*,
 642 abs/2503.09516, 2025. doi: 10.48550/ARXIV.2503.09516. URL <https://doi.org/10.48550/arXiv.2503.09516>.

645 Aishwarya Kamath, Johan Ferret, Shreya Pathak, Nino Vieillard, Ramona Merhej, Sarah Perrin, Ta-
 646 tiana Matejovicova, Alexandre Ramé, Morgane Rivière, Louis Rouillard, Thomas Mesnard, Geof-
 647 frey Cideron, Jean-Bastien Grill, Sabela Ramos, Edouard Yvinec, Michelle Casbon, Etienne Pot,
 Ivo Penchev, Gaël Liu, Francesco Visin, Kathleen Kenealy, Lucas Beyer, Xiaohai Zhai, Anton

648 Tsitsulin, Róbert Busa-Fekete, Alex Feng, Noveen Sachdeva, Benjamin Coleman, Yi Gao, Basil
 649 Mustafa, Iain Barr, Emilio Parisotto, David Tian, Matan Eyal, Colin Cherry, Jan-Thorsten Peter,
 650 Danila Sinopalnikov, Surya Bhupatiraju, Rishabh Agarwal, Mehran Kazemi, Dan Malkin, Ravin
 651 Kumar, David Vilar, Idan Brusilovsky, Jiaming Luo, Andreas Steiner, Abe Friesen, Abhanshu
 652 Sharma, Abheesht Sharma, Adi Mayrav Gilady, Adrian Goedeckemeyer, Alaa Saade, Alexan-
 653 der Kolesnikov, Alexei Bendebury, Alvin Abdagic, Amit Vadi, András György, André Susano
 654 Pinto, Anil Das, Ankur Bapna, Antoine Miech, Antoine Yang, Antonia Paterson, Ashish Shenoy,
 655 Ayan Chakrabarti, Bilal Piot, Bo Wu, Bobak Shahriari, Bryce Petrini, Charlie Chen, Charline Le
 656 Lan, Christopher A. Choquette-Choo, CJ Carey, Cormac Brick, Daniel Deutscher, Danielle Eisen-
 657 bud, Dee Cattle, Derek Cheng, Dimitris Paparas, Divyashree Shivakumar Sreepathihalli, Doug
 658 Reid, Dustin Tran, Dustin Zelle, Eric Noland, Erwin Huizenga, Eugene Kharitonov, Frederick
 659 Liu, Gagik Amirkhanyan, Glenn Cameron, Hadi Hashemi, Hanna Klimczak-Plucinska, Harman
 660 Singh, Harsh Mehta, Harshal Tushar Lehri, Hussein Hazimeh, Ian Ballantyne, Idan Szektor, and
 661 Ivan Nardini. Gemma 3 technical report. *CoRR*, abs/2503.19786, 2025. doi: 10.48550/ARXIV.
 662 2503.19786. URL <https://doi.org/10.48550/arXiv.2503.19786>.

663 Xin Lai, Junyi Li, Wei Li, Tao Liu, Tianjian Li, and Hengshuang Zhao. Mini-o3: Scaling up
 664 reasoning patterns and interaction turns for visual search, 2025. URL <https://arxiv.org/abs/2509.07969>.

665 Kaixin Li, Yuchen Tian, Qisheng Hu, Ziyang Luo, Zhiyong Huang, and Jing Ma. Mmcode:
 666 Benchmarking multimodal large language models for code generation with visually rich pro-
 667 gramming problems. In Yaser Al-Onaizan, Mohit Bansal, and Yun-Nung Chen (eds.), *Find-
 668 ings of the Association for Computational Linguistics: EMNLP 2024, Miami, Florida, USA,
 669 November 12-16, 2024*, pp. 736–783. Association for Computational Linguistics, 2024. doi: 10.
 670 18653/V1/2024.FINDINGS-EMNLP.42. URL <https://doi.org/10.18653/v1/2024.findings-emnlp.42>.

671 Xuefeng Li, Haoyang Zou, and Pengfei Liu. Torl: Scaling tool-integrated RL. *CoRR*,
 672 abs/2503.23383, 2025. doi: 10.48550/ARXIV.2503.23383. URL <https://doi.org/10.48550/arXiv.2503.23383>.

673 Heng Lin and Zhongwen Xu. Understanding tool-integrated reasoning, 2025. URL <https://arxiv.org/abs/2508.19201>.

674 Pan Lu, Hritik Bansal, Tony Xia, Jiacheng Liu, Chunyuan Li, Hannaneh Hajishirzi, Hao Cheng, Kai-
 675 Wei Chang, Michel Galley, and Jianfeng Gao. Mathvista: Evaluating mathematical reasoning
 676 of foundation models in visual contexts. In *The Twelfth International Conference on Learning
 677 Representations, ICLR 2024, Vienna, Austria, May 7-11, 2024*. OpenReview.net, 2024. URL
 678 <https://openreview.net/forum?id=KUNzEQMWU7>.

679 Pan Lu, Bowen Chen, Sheng Liu, Rahul Thapa, Joseph Boen, and James Zou. Octotools: An agentic
 680 framework with extensible tools for complex reasoning. *CoRR*, abs/2502.11271, 2025. doi: 10.
 681 48550/ARXIV.2502.11271. URL <https://doi.org/10.48550/arXiv.2502.11271>.

682 Fanqing Meng, Lingxiao Du, Zongkai Liu, Zhixiang Zhou, Quanfeng Lu, Daocheng Fu, Bo-
 683 tian Shi, Wenhui Wang, Junjun He, Kaipeng Zhang, Ping Luo, Yu Qiao, Qiaosheng Zhang,
 684 and Wenqi Shao. Mm-eureka: Exploring visual aha moment with rule-based large-scale rein-
 685 forcement learning. *CoRR*, abs/2503.07365, 2025. doi: 10.48550/ARXIV.2503.07365. URL
 686 <https://doi.org/10.48550/arXiv.2503.07365>.

687 OpenAI. Hello gpt-4o, 2024. URL <https://openai.com/index/hello-gpt-4o/>.

688 OpenAI. Introducing openai o3 and o4-mini. <https://openai.com/index/introducing-o3-and-o4-mini/>, 2025a.

689 OpenAI. Gpt-4.1. <https://openai.com/index/gpt-4-1/>, 2025b.

690 Yueqi Song, Tianyue Ou, Yibo Kong, Zecheng Li, Graham Neubig, and Xiang Yue. Visualpuzzles:
 691 Decoupling multimodal reasoning evaluation from domain knowledge. *CoRR*, abs/2504.10342,
 692 2025. doi: 10.48550/ARXIV.2504.10342. URL <https://doi.org/10.48550/arXiv.2504.10342>.

702 Alex Su, Haozhe Wang, Weiming Ren, Fangzhen Lin, and Wenhui Chen. Pixel reasoner: Incentivizing
 703 pixel-space reasoning with curiosity-driven reinforcement learning. *CoRR*, abs/2505.15966,
 704 2025a. doi: 10.48550/ARXIV.2505.15966. URL <https://doi.org/10.48550/arXiv.2505.15966>.

705

706 Zhaochen Su, Linjie Li, Mingyang Song, Yunzhuo Hao, Zhengyuan Yang, Jun Zhang, Guanjie
 707 Chen, Jiawei Gu, Juntao Li, Xiaoye Qu, and Yu Cheng. Openthinkimg: Learning to think with
 708 images via visual tool reinforcement learning. *CoRR*, abs/2505.08617, 2025b. doi: 10.48550/
 709 ARXIV.2505.08617. URL <https://doi.org/10.48550/arXiv.2505.08617>.

710

711 Zhaochen Su, Peng Xiang, Hangyu Guo, Zhenhua Liu, Yan Ma, Xiaoye Qu, Jiaqi Liu, Yanshu Li,
 712 Kaide Zeng, Zhengyuan Yang, Linjie Li, Yu Cheng, Heng Ji, Junxian He, and Yi R. (May) Fung.
 713 Thinking with images for multimodal reasoning: Foundations, methods, and future frontiers.
 714 *CoRR*, abs/2506.23918, 2025c. doi: 10.48550/ARXIV.2506.23918. URL <https://doi.org/10.48550/arXiv.2506.23918>.

715

716 Dídac Surís, Sachit Menon, and Carl Vondrick. Vipergrt: Visual inference via python execution
 717 for reasoning. In *IEEE/CVF International Conference on Computer Vision, ICCV 2023, Paris,
 718 France, October 1-6, 2023*, pp. 11854–11864. IEEE, 2023. doi: 10.1109/ICCV51070.2023.
 719 01092. URL <https://doi.org/10.1109/ICCV51070.2023.01092>.

720

721 Bohao Tang, Yan Ma, Fei Zhang, Jiadi Su, Ethan Chern, Zhulin Hu, Zhixin Wang, Pengfei Liu, and
 722 Ya Zhang. Visual programmability: A guide for code-as-thought in chart understanding, 2025.
 723 URL <https://arxiv.org/abs/2509.09286>.

724

725 Ke Wang, Junting Pan, Weikang Shi, Zimu Lu, Houxing Ren, Aojun Zhou, Mingjie Zhan, and
 726 Hongsheng Li. Measuring multimodal mathematical reasoning with math-vision dataset. In Amir
 727 Globersons, Lester Mackey, Danielle Belgrave, Angela Fan, Ulrich Paquet, Jakub M. Tomczak,
 728 and Cheng Zhang (eds.), *Advances in Neural Information Processing Systems 38: Annual
 729 Conference on Neural Information Processing Systems 2024, NeurIPS 2024, Vancouver, BC, Canada,
 730 December 10 - 15, 2024*, 2024. URL http://papers.nips.cc/paper_files/paper/2024/hash/ad0edc7d5fa1a783f063646968b7315b-Abstract-Datasets_and_Benchmarks_Track.html.

731

732

733 Ke Wang, Junting Pan, Linda Wei, Aojun Zhou, Weikang Shi, Zimu Lu, Han Xiao, Yunqiao Yang,
 734 Houxing Ren, Mingjie Zhan, and Hongsheng Li. Mathcoder-vl: Bridging vision and code for
 735 enhanced multimodal mathematical reasoning. In Wanxiang Che, Joyce Nabende, Ekaterina
 736 Shutova, and Mohammad Taher Pilehvar (eds.), *Findings of the Association for Computational
 737 Linguistics, ACL 2025, Vienna, Austria, July 27 - August 1, 2025*, pp. 2505–2534. Association
 738 for Computational Linguistics, 2025a. URL <https://aclanthology.org/2025.findings-acl.128/>.

739

740 Weiyun Wang, Zhangwei Gao, Lixin Gu, Hengjun Pu, Long Cui, Xingguang Wei, Zhaoyang
 741 Liu, Linglin Jing, Shenglong Ye, Jie Shao, Zhaokai Wang, Zhe Chen, Hongjie Zhang, Ganlin
 742 Yang, Haomin Wang, Qi Wei, Jinhui Yin, Wenhao Li, Erfei Cui, Guanzhou Chen, Zichen Ding,
 743 Changyao Tian, Zhenyu Wu, JingJing Xie, Zehao Li, Bowen Yang, Yuchen Duan, Xuehui Wang,
 744 Zhi Hou, Haoran Hao, Tianyi Zhang, Songze Li, Xiangyu Zhao, Haodong Duan, Nianchen Deng,
 745 Bin Fu, Yinan He, Yi Wang, Conghui He, Botian Shi, Junjun He, Yingtong Xiong, Han Lv, Lijun
 746 Wu, Wenqi Shao, Kaipeng Zhang, Huipeng Deng, Biqing Qi, Jiaye Ge, Qipeng Guo, Wenwei
 747 Zhang, Songyang Zhang, Maosong Cao, Junyao Lin, Kexian Tang, Jianfei Gao, Haian Huang,
 748 Yuzhe Gu, Chengqi Lyu, Huanze Tang, Rui Wang, Haijun Lv, Wanli Ouyang, Limin Wang, Min
 749 Dou, Xizhou Zhu, Tong Lu, Dahua Lin, Jifeng Dai, Weijie Su, Bowen Zhou, Kai Chen, Yu Qiao,
 750 Wenhui Wang, and Gen Luo. Internvl3.5: Advancing open-source multimodal models in versatility,
 751 reasoning, and efficiency. *CoRR*, abs/2508.18265, 2025b. doi: 10.48550/ARXIV.2508.18265.
 752 URL <https://doi.org/10.48550/arXiv.2508.18265>.

753

754 Xiya Wang, Zhengyuan Yang, Chao Feng, Hongjin Lu, Linjie Li, Chung-Ching Lin, Kevin Lin,
 755 Furong Huang, and Lijuan Wang. Sota with less: Mcts-guided sample selection for data-efficient
 756 visual reasoning self-improvement. *CoRR*, abs/2504.07934, 2025c. doi: 10.48550/ARXIV.2504.
 07934. URL <https://doi.org/10.48550/arXiv.2504.07934>.

756 Ye Wang, Qianglong Chen, Zejun Li, Siyuan Wang, Shijie Guo, Zhirui Zhang, and Zhongyu Wei.
 757 Simple o3: Towards interleaved vision-language reasoning, 2025d. URL <https://arxiv.org/abs/2508.12109>.
 758

760 Jason Wei, Xuezhi Wang, Dale Schuurmans, Maarten Bosma, Brian Ichter, Fei Xia, Ed H. Chi,
 761 Quoc V. Le, and Denny Zhou. Chain-of-thought prompting elicits reasoning in large language
 762 models. In Sanmi Koyejo, S. Mohamed, A. Agarwal, Danielle Belgrave, K. Cho, and A. Oh
 763 (eds.), *Advances in Neural Information Processing Systems 35: Annual Conference on Neural
 764 Information Processing Systems 2022, NeurIPS 2022, New Orleans, LA, USA, November 28 - De-
 765 cember 9, 2022*, 2022. URL [http://papers.nips.cc/paper_files/paper/2022/
 766 hash/9d5609613524ecf4f15af0f7b31abca4-Abstract-Conference.html](http://papers.nips.cc/paper_files/paper/2022/hash/9d5609613524ecf4f15af0f7b31abca4-Abstract-Conference.html).
 767

768 Chao Wen, Jacqueline Staub, and Adish Singla. Program synthesis benchmark for visual program-
 769 ming in XLogoOnline environment. In Wanxiang Che, Joyce Nabende, Ekaterina Shutova, and
 770 Mohammad Taher Pilehvar (eds.), *Proceedings of the 63rd Annual Meeting of the Association
 771 for Computational Linguistics (Volume 1: Long Papers)*, pp. 15812–15838, Vienna, Austria, July
 772 2025. Association for Computational Linguistics. ISBN 979-8-89176-251-0. doi: 10.18653/v1/
 773 2025.acl-long.769. URL <https://aclanthology.org/2025.acl-long.769>.
 774

775 Fang Wu, Weihao Xuan, Ximing Lu, Zaïd Harchaoui, and Yejin Choi. The invisible leash: Why
 776 RLVR may not escape its origin. *CoRR*, abs/2507.14843, 2025a. doi: 10.48550/ARXIV.2507.
 777 14843. URL <https://doi.org/10.48550/arXiv.2507.14843>.
 778

779 Junfei Wu, Jian Guan, Kaituo Feng, Qiang Liu, Shu Wu, Liang Wang, Wei Wu, and Tieniu
 780 Tan. Reinforcing spatial reasoning in vision-language models with interwoven thinking and
 781 visual drawing. *CoRR*, abs/2506.09965, 2025b. doi: 10.48550/ARXIV.2506.09965. URL
 782 <https://doi.org/10.48550/arXiv.2506.09965>.
 783

784 Zhenghai Xue, Longtao Zheng, Qian Liu, Yingru Li, Xiaosen Zheng, Zejun Ma, and Bo An. Sim-
 785 pletir: End-to-end reinforcement learning for multi-turn tool-integrated reasoning, 2025. URL
 786 <https://arxiv.org/abs/2509.02479>.
 787

788 Biao Yang, Bin Wen, Boyang Ding, Changyi Liu, Chenglong Chu, Chengru Song, Chongling Rao,
 789 Chuan Yi, Da Li, Dunju Zang, Fan Yang, Guorui Zhou, Guowang Zhang, Han Shen, Hao Peng,
 790 Haojie Ding, Hao Wang, Haonan Fan, Hengrui Ju, Jiaming Huang, Jiangxia Cao, Jiankang Chen,
 791 Jingyun Hua, Kaibing Chen, Kaiyu Jiang, Kaiyu Tang, Kun Gai, Muham Wei, Qiang Wang, Ruitao
 792 Wang, Sen Na, Shengnan Zhang, Siyang Mao, Sui Huang, Tianke Zhang, Tingting Gao, Wei
 793 Chen, Wei Yuan, Xiangyu Wu, Xiao Hu, Xingyu Lu, Yi-Fan Zhang, Yiping Yang, Yulong Chen,
 794 Zeyi Lu, Zhenhua Wu, Zhixin Ling, Zhuoran Yang, Ziming Li, Di Xu, Haixuan Gao, Hang Li,
 795 Jing Wang, Lejian Ren, Qigen Hu, Qianqian Wang, Shiyao Wang, Xinchen Luo, Yan Li, Yuhang
 796 Hu, and Zixing Zhang. Kwai keye-vl 1.5 technical report, 2025a. URL <https://arxiv.org/abs/2509.01563>.
 797

798 John Yang, Carlos E. Jimenez, Alex L. Zhang, Kilian Lieret, Joyce Yang, Xindi Wu, Ori Press,
 799 Niklas Muennighoff, Gabriel Synnaeve, Karthik R. Narasimhan, Diyi Yang, Sida Wang, and
 800 Ofir Press. Swe-bench multimodal: Do AI systems generalize to visual software domains? In
 801 *The Thirteenth International Conference on Learning Representations, ICLR 2025, Singapore,
 802 April 24-28, 2025*. OpenReview.net, 2025b. URL <https://openreview.net/forum?id=riTiq3i21b>.
 803

804 Xiang Yue, Yuansheng Ni, Tianyu Zheng, Kai Zhang, Ruoqi Liu, Ge Zhang, Samuel Stevens,
 805 Dongfu Jiang, Weiming Ren, Yuxuan Sun, Cong Wei, Bota Yu, Ruibin Yuan, Renliang Sun,
 806 Ming Yin, Boyuan Zheng, Zhenzhu Yang, Yibo Liu, Wenhao Huang, Huan Sun, Yu Su, and
 807 Wenhui Chen. MMMU: A massive multi-discipline multimodal understanding and reason-
 808 ing benchmark for expert AGI. In *IEEE/CVF Conference on Computer Vision and Pattern
 809 Recognition, CVPR 2024, Seattle, WA, USA, June 16-22, 2024*, pp. 9556–9567. IEEE, 2024.
 810 doi: 10.1109/CVPR52733.2024.00913. URL <https://doi.org/10.1109/CVPR52733.2024.00913>.
 811

812 Fengji Zhang, Linquan Wu, Huiyu Bai, Guancheng Lin, Xiao Li, Xiao Yu, Yue Wang, Bei Chen,
 813 and Jacky Keung. Humaneval-v: Evaluating visual understanding and reasoning abilities of large
 814

810 multimodal models through coding tasks. *CoRR*, abs/2410.12381, 2024a. doi: 10.48550/ARXIV.
 811 2410.12381. URL <https://doi.org/10.48550/arXiv.2410.12381>.

812

813 Renrui Zhang, Dongzhi Jiang, Yichi Zhang, Haokun Lin, Ziyu Guo, Pengshuo Qiu, Aojun Zhou,
 814 Pan Lu, Kai-Wei Chang, Yu Qiao, Peng Gao, and Hongsheng Li. MATHVERSE: does your
 815 multi-modal LLM truly see the diagrams in visual math problems? In Ales Leonardis, Elisa
 816 Ricci, Stefan Roth, Olga Russakovsky, Torsten Sattler, and G  l Varol (eds.), *Computer Vi-
 817 sion - ECCV 2024 - 18th European Conference, Milan, Italy, September 29-October 4, 2024,
 818 Proceedings, Part VIII*, volume 15066 of *Lecture Notes in Computer Science*, pp. 169-186.
 819 Springer, 2024b. doi: 10.1007/978-3-031-73242-3\10. URL https://doi.org/10.1007/978-3-031-73242-3_10.

820

821 Yifan Zhang, Xingyu Lu, Shukang Yin, Chaoyou Fu, Wei Chen, Xiao Hu, Bin Wen, Kaiyu Jiang,
 822 Changyi Liu, Tianke Zhang, Haonan Fan, Kaibing Chen, Jiankang Chen, Haojie Ding, Kaiyu
 823 Tang, Zhang Zhang, Liang Wang, Fan Yang, Tingting Gao, and Guorui Zhou. Thyme: Think
 824 beyond images. *CoRR*, abs/2508.11630, 2025. doi: 10.48550/ARXIV.2508.11630. URL <https://doi.org/10.48550/arXiv.2508.11630>.

825

826 Zhuosheng Zhang, Aston Zhang, Mu Li, Hai Zhao, George Karypis, and Alex Smola. Multimodal
 827 chain-of-thought reasoning in language models. *Trans. Mach. Learn. Res.*, 2024, 2024c. URL
 828 <https://openreview.net/forum?id=y1pPWFVfvR>.

829

830 Shitian Zhao, Haoquan Zhang, Shaoheng Lin, Ming Li, Qilong Wu, Kaipeng Zhang, and Chen Wei.
 831 Pyvision: Agentic vision with dynamic tooling, 2025. URL <https://arxiv.org/abs/2507.07998>.

832

833 Ziwei Zheng, Michael Yang, Jack Hong, Chenxiao Zhao, Guohai Xu, Le Yang, Chao Shen, and
 834 Xing Yu. Deepeyes: Incentivizing "thinking with images" via reinforcement learning. *CoRR*,
 835 abs/2505.14362, 2025. doi: 10.48550/ARXIV.2505.14362. URL <https://doi.org/10.48550/arXiv.2505.14362>.

836

837 Zetong Zhou, Dongping Chen, Zixian Ma, Zhihan Hu, Mingyang Fu, Sinan Wang, Yao Wan, Zhou
 838 Zhao, and Ranjay Krishna. Reinforced visual perception with tools, 2025. URL <https://arxiv.org/abs/2509.01656>.

840

841

842

843

844

845

846

847

848

849

850

851

852

853

854

855

856

857

858

859

860

861

862

863

864 **A LLM USAGE STATEMENT**
865866 In this work, Large Language Models (LLMs) were used solely as general-purpose auxiliary tools.
867 Their role was limited to polishing grammar and phrasing to enhance the clarity of the manuscript,
868 as well as assisting in the generation of Python and LaTeX code for creating figures and tables. No
869 parts of the research ideation, experimental design, analysis, or substantive writing relied on LLMs.
870871 **B DISCUSSION**
872873 Here, we would like to discuss the relationship between Thinking with Images (TWI) and Thinking
874 with Visual Programming (TVP).
875876 Existing approaches under the Thinking with Images paradigm typically rely on a predefined set of
877 visual tools, such as cropping, zooming, and rotating. These operations can indeed enhance per-
878 ceptual accuracy, especially for handling high-resolution images or focusing attention on relevant
879 regions. However, their scope is inherently narrow. While effective for improving low-level per-
880 ception, such fixed transformations provide limited support for deep reasoning tasks that require
881 abstraction, planning, or algorithmic optimization. In other words, current Thinking with Images
882 primarily enhances *seeing more carefully*, but does not necessarily enable *thinking more deeply*.
883884 In contrast, Thinking with Visual Programming generalizes beyond fixed toolkits by allowing mod-
885 els to write and execute code, thus treating visual operations themselves as programmable functions.
886 This enables not only flexible tool selection but also the creation of new tools on demand, allowing
887 the reasoning process to adapt dynamically to the task at hand. Under this view, cropping or rotat-
888 ing an image represents only one instance within a broader spectrum of programmable operations,
889 which may also involve algorithmic simulation, complex computation, or visualization.
890891 From this perspective, TWI can be regarded as a subset of TVP, serving as a valuable stepping stone
892 but not the ultimate goal. As our experimental results demonstrate, current models remain far from
893 fully realizing the TVP paradigm. While existing studies have already achieved promising outcomes
894 under the TWI framework, a substantial gap persists between these methods and the broader vision
895 of TVP. Bridging this gap requires equipping models with stronger visual programming capabili-
896 ties and more advanced visual abstraction skills, enabling them to move beyond fixed perceptual
897 tools toward flexible, programmable reasoning. On this foundation, agentic reinforcement learning
898 can become truly effective. In the future, we envision equipping MLLMs with access to external
899 resources such as web browsers. This would allow them not only to autonomously create tools
900 through code but also to search for and integrate existing tools from the internet.
901902
903
904
905
906
907
908
909
910
911
912
913
914
915
916
917

918 C BENCHMARK DETAILS
919920 To ensure the data quality of MMR-VIP, we provided annotators with a detailed guideline:
921

922 All tasks must:

923 (1) Be code-synthesizable (problems, images, and solutions are generated by code).
 924 (2) Be aligned with cognitive skills (at least 1, at most 3 from the given taxonomy).
 925 (3) Be stratified into difficulty levels (Easy / Medium / Hard).
 926 (4) Be suitable for programmatic reasoning (problems solvable or aided by code execution).

927 **Cognitive Skills**

928 (1) Attribute: identify colors, shapes, sizes.
 929 (2) Location: detect positions, distances, spatial relations.
 930 (3) Symbolic: recognize digits, letters, or visual symbols.
 931 (4) Geometry: formulate geometric equations or relations.
 932 (5) Physics: model dynamics using physical laws.
 933 (6) Network: construct graph structures (nodes, edges, constraints).
 934 (7) Search: implement DFS, BFS, or other exploration methods.
 935 (8) Planning: apply dynamic/linear programming to solve constrained problems.
 936 (9) Computation: perform numerical calculations or algorithmic procedures.

936 **Difficulty Levels**

937 (1) Easy: solvable using intrinsic perceptual and reasoning abilities, without code execution.
 938 (2) Medium: requiring programmatic operations, where external computation is essential.
 939 (3) Hard: remaining challenging even with programming support, typically due to high algo-
 940 rithmic complexity or intricate constraints.

940 **Workflow**

941 Annotators should first define the problem (including its target cognitive skills and difficulty
 942 levels), then implement code that generates instances and computes the ground-truth solution.
 943 Next, the problem must be visualized using standard libraries to ensure clarity. Each program
 944 should support batch generation of images, questions, and answers across difficulty levels.
 945 Finally, the generated code must undergo validation, where outputs are independently reviewed
 946 to ensure correctness and consistency between problem, visualization, and answer.

Hanoi Tower (Attribute)		
		
Question: Find the minimum number of moves required to get from the Tower of Hanoi state described in the figure to the completed state. Answer: 28	Question: Find the minimum number of moves required to get from the Tower of Hanoi state described in the figure to the completed state. Answer: 52	Question: Find the minimum number of moves required to get from the Tower of Hanoi state described in the figure to the completed state. Answer: 26
Difficulty: Easy	Difficulty: Medium	Difficulty: Hard

958 Figure 7: Data example of Hanoi Tower.
959

Sliding Puzzle (Search)		
		
Question: At each time, any colored ball can be exchanged with the white ball. How many such exchanges are needed at least to make all the red balls arranged in front of the green balls (white ball positions are arbitrary)? Answer: 5	Question: At each time, any colored ball can be exchanged with the white ball. How many such exchanges are needed at least to make all the red balls arranged in front of the green balls (white ball positions are arbitrary)? Answer: 9	Question: At each time, any colored ball can be exchanged with the white ball. How many such exchanges are needed at least to make all the red balls arranged in front of the blue balls and blue balls in front of the yellow balls (white ball positions are arbitrary)? Answer: 9
Difficulty: Easy	Difficulty: Medium	Difficulty: Hard

968 Figure 8: Data example of Sliding Puzzle.
969

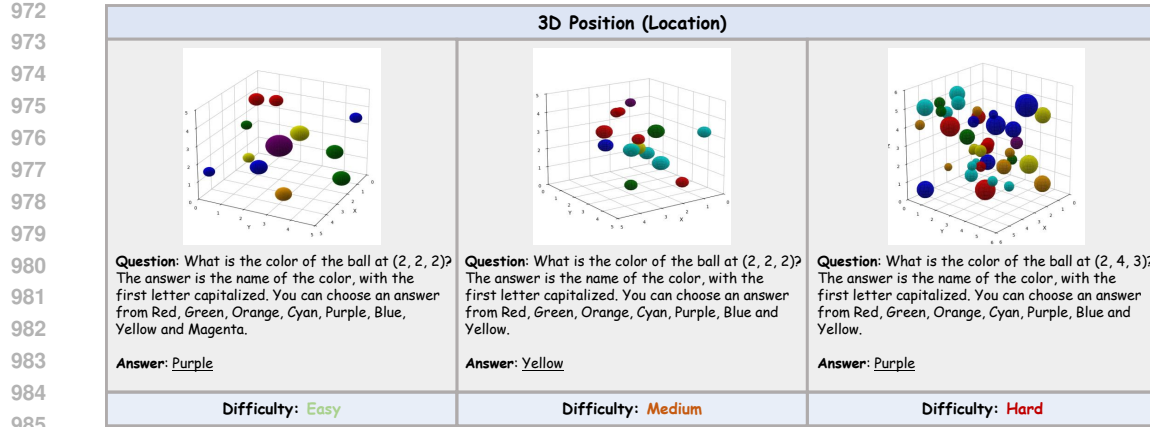


Figure 9: Data example of 3D Position.

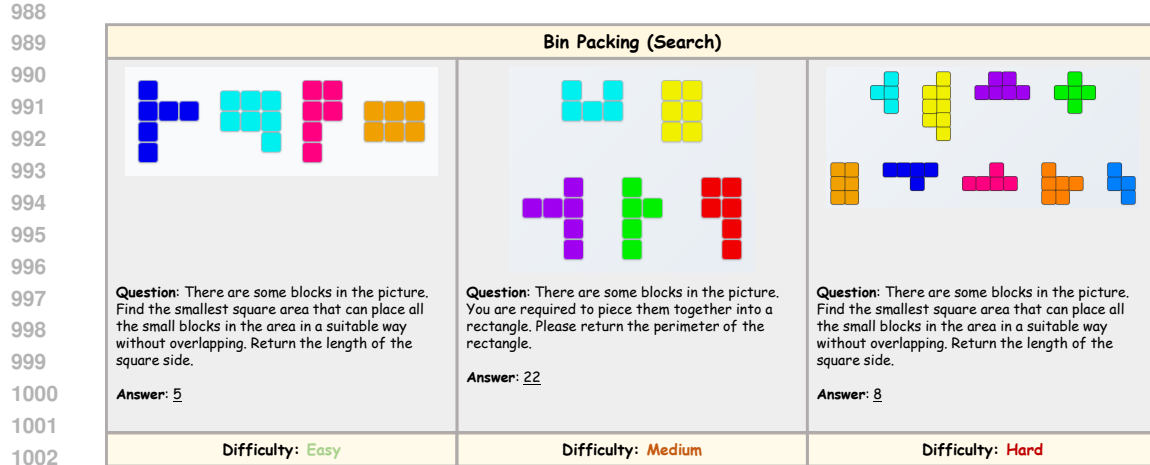


Figure 10: Data example of Bin Packing.

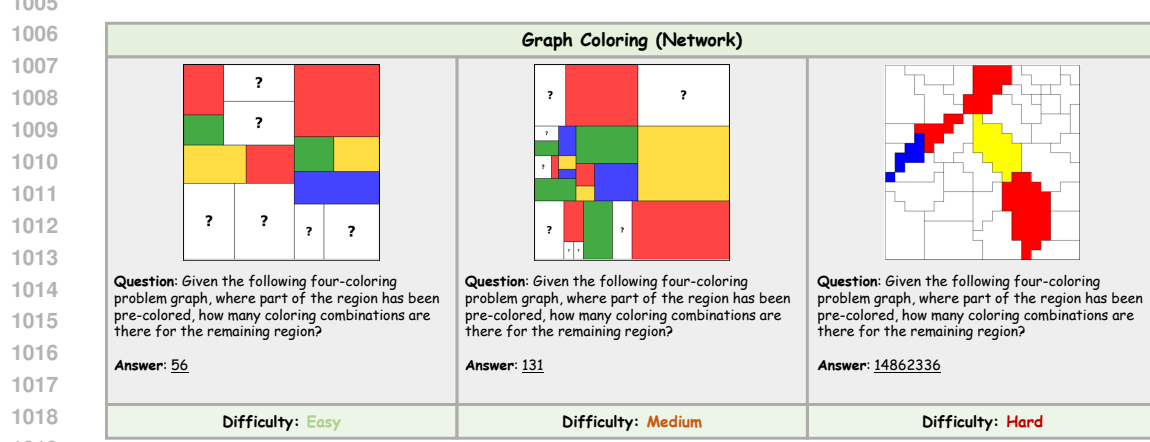


Figure 11: Data example of Graph Coloring.

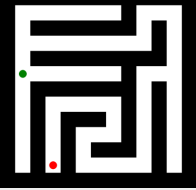
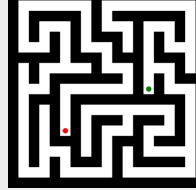
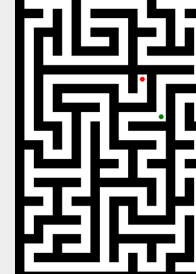
Maze (Search)		
		
<p>Question: The picture describes a maze problem, where green is the starting position and red is the end point. Find the length of the shortest path. Each grid square has a length of 1.</p> <p>Answer: <u>44</u></p>	<p>Question: The picture describes a maze problem, where green is the starting position and red is the end point. Find the length of the shortest path. Each grid square has a length of 1.</p> <p>Answer: <u>104</u></p>	<p>Question: The picture describes a maze problem, where green is the starting position and red is the end point. Find the length of the shortest path. Each grid square has a length of 1.</p> <p>Answer: <u>102</u></p>
Difficulty: Easy	Difficulty: Medium	Difficulty: Hard

Figure 12: Data example of Maze.

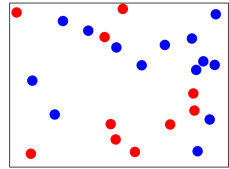
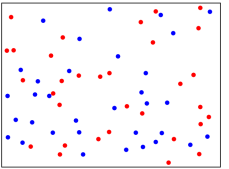
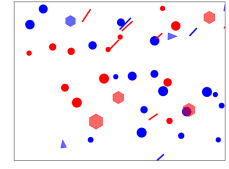
Point Counting (Attribute)		
		
<p>Question: What is the number of red dots?</p> <p>Answer: <u>10</u></p>	<p>Question: What is the number of red dots?</p> <p>Answer: <u>32</u></p>	<p>Question: What is the number of red dots?</p> <p>Answer: <u>12</u></p>
Difficulty: Easy	Difficulty: Medium	Difficulty: Hard

Figure 13: Data example of Point Counting.

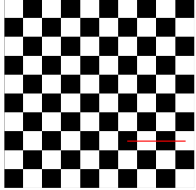
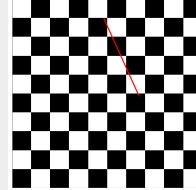
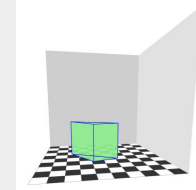
Height Measurement (Location)		
		
<p>Question: Detect the length of the red line, where the side length of each grid on the chessboard is 0.5. The length of the red line is an integer multiple of the length of the floor tile. How long is the red line in the picture?</p> <p>Answer: <u>1.5</u></p>	<p>Question: Detect the diagonal length of the red line, where the side length of each grid square is 0.5. The result should be rounded to one decimal place.</p> <p>Answer: <u>2.2</u></p>	<p>Question: Estimate the volume of the 3D prism shown in the image. The result should be rounded to one decimal place. The side length of each grid on the chessboard is 0.5.</p> <p>Answer: <u>1.3</u></p>
Difficulty: Easy	Difficulty: Medium	Difficulty: Hard

Figure 14: Data example of Height Measurement.

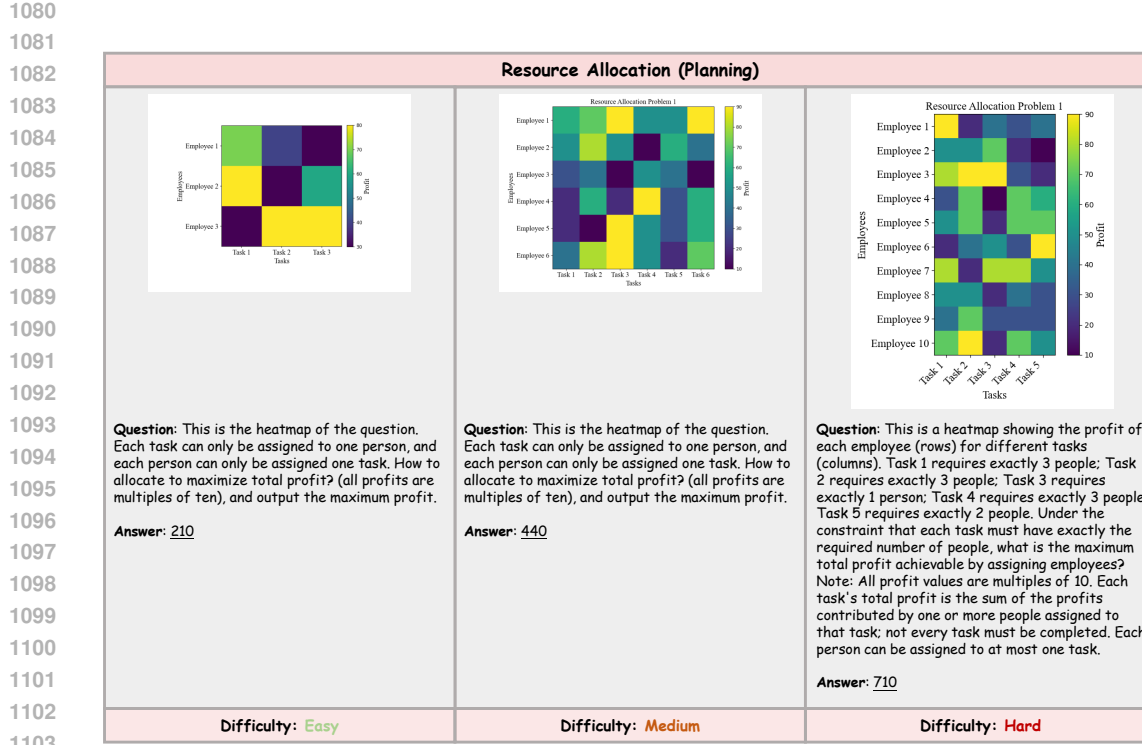


Figure 15: Data example of Resource Allocation.

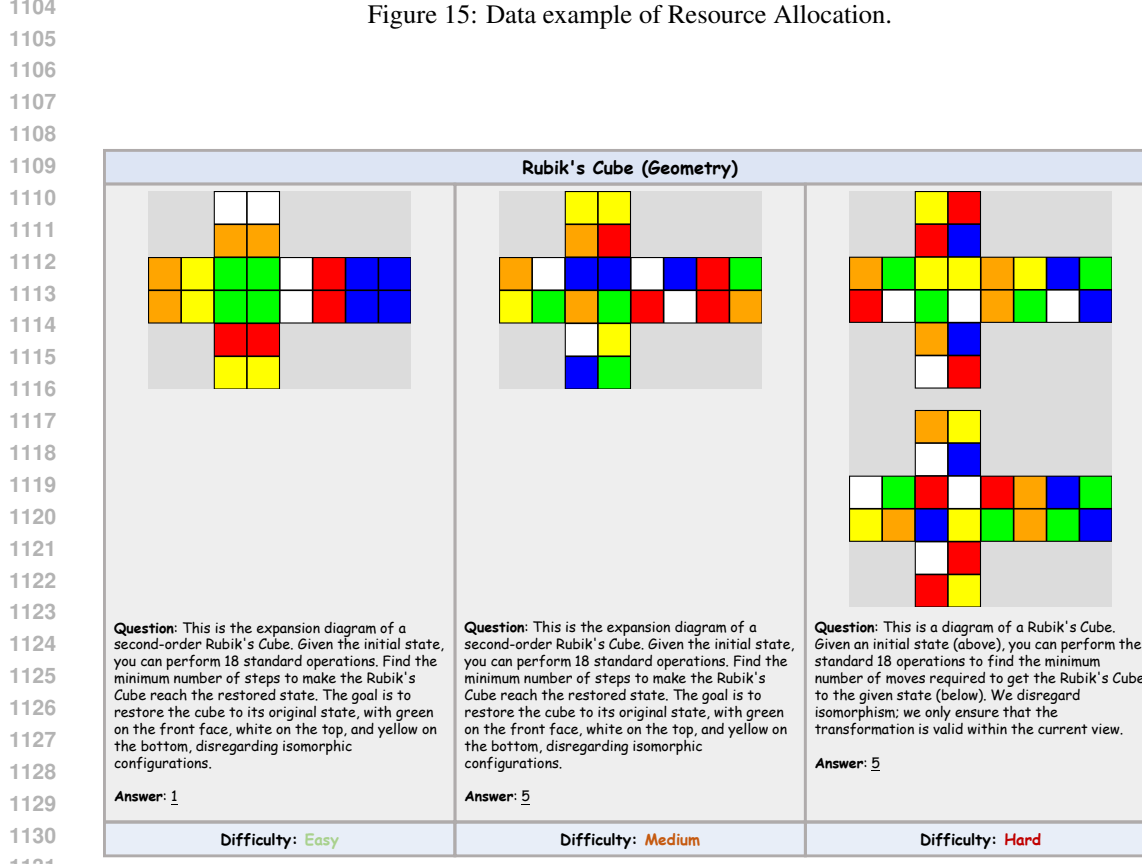


Figure 16: Data example of Rubik's Cube.

Lights Out (Planning)		
<p>Question: Game Rule: Clicking a light toggles itself and its adjacent (up, down, left, right) lights. What is the minimum number of clicks required to turn off all the lights?</p> <p>Answer: <u>2</u></p>	<p>Question: Game Rule: Clicking a light toggles itself and its adjacent (up, down, left, right) lights. What is the minimum number of clicks required to turn off all the lights?</p> <p>Answer: <u>6</u></p>	<p>Question: Game Rule: Clicking a light toggles itself and its diagonal (upper-left, upper-right, lower-left, lower-right) lights. What is the minimum number of clicks required to turn off all the lights?</p> <p>Answer: <u>12</u></p>
Difficulty: Easy	Difficulty: Medium	Difficulty: Hard

Figure 17: Data example of Lights Out.

Snake Game (Search)		
<p>Question: This is a snake game. How many steps do you need to take from the current state to eat the food?</p> <p>Answer: <u>6</u></p>	<p>Question: This is a snake game. How many steps do you need to take from the current state to eat two foods one after another (regardless of the order of the two foods)?</p> <p>Answer: <u>13</u></p>	<p>Question: This is a snake game. How many steps do you need to take from the current state to eat two foods one after another (regardless of the order of the two foods)? At the same time, pay attention to avoid obstacles.</p> <p>Answer: <u>10</u></p>
Difficulty: Easy	Difficulty: Medium	Difficulty: Hard

Figure 18: Data example of Snake Game.

Three-Views (Geometry)		
<p>Question: Given a description of the three-view drawing of a solid figure, find the maximum number of small cubes that the solid figure can be composed of when the three-view constraints are met.</p> <p>Answer: <u>7</u></p>	<p>Question: Given a description of the three-view drawing of a solid figure, find the maximum number of small cubes that the solid figure can be composed of when the three-view constraints are met.</p> <p>Answer: <u>13</u></p>	<p>Question: Given a description of the three-view drawing of a solid figure, find the maximum number of small cubes that the solid figure can be composed of when the three-view constraints are met.</p> <p>Answer: <u>25</u></p>
Difficulty: Easy	Difficulty: Medium	Difficulty: Hard

Figure 19: Data example of Three-Views.

1188

1189

1190

1191

1192

1193

1194

1195

1196

1197

1198

1199

1200

1201

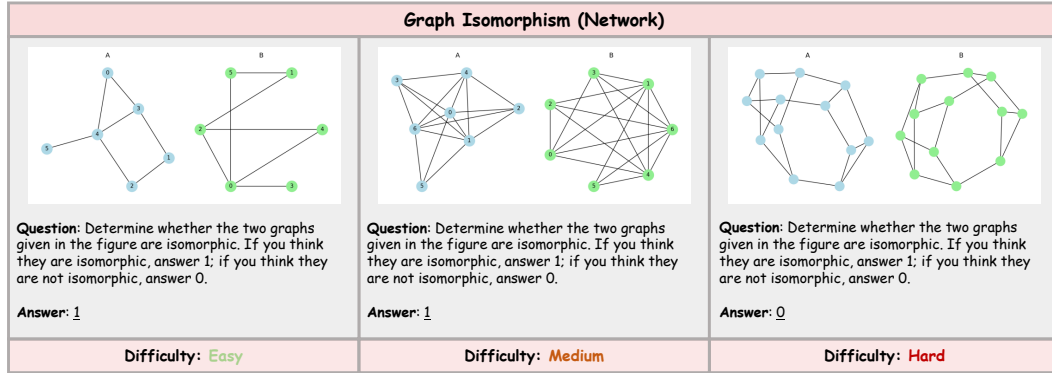


Figure 20: Data example of Graph Isomorphism.

1202

1203

1204

1205

1206

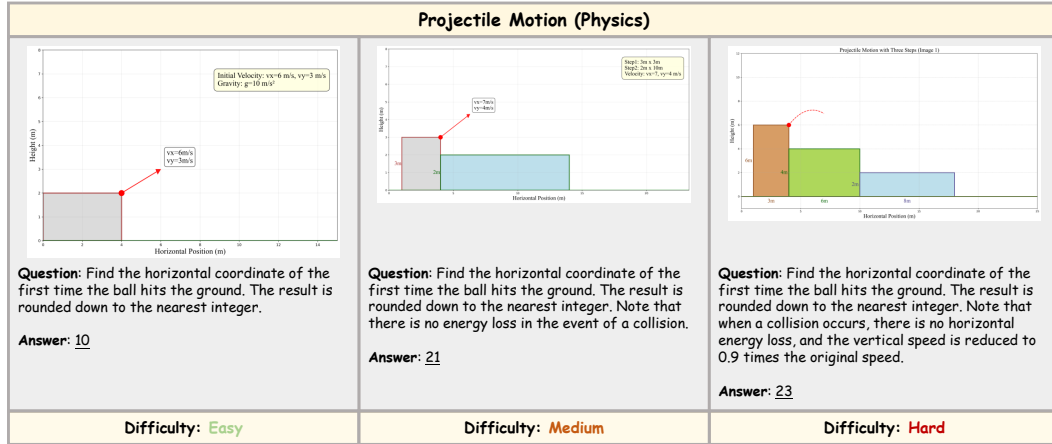


Figure 21: Data example of Projectile Motion.

1221

1222

1223

1224

1225

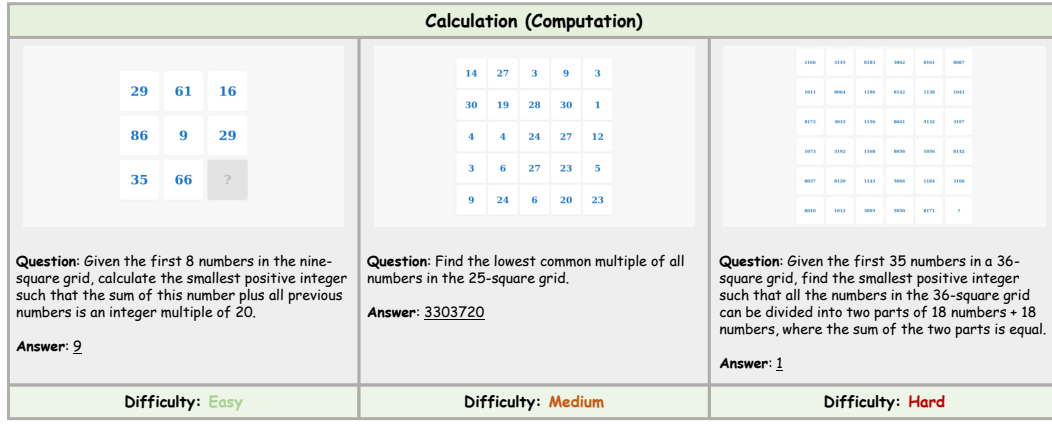


Figure 22: Data example of Calculation.

1238

1239

1240

1241

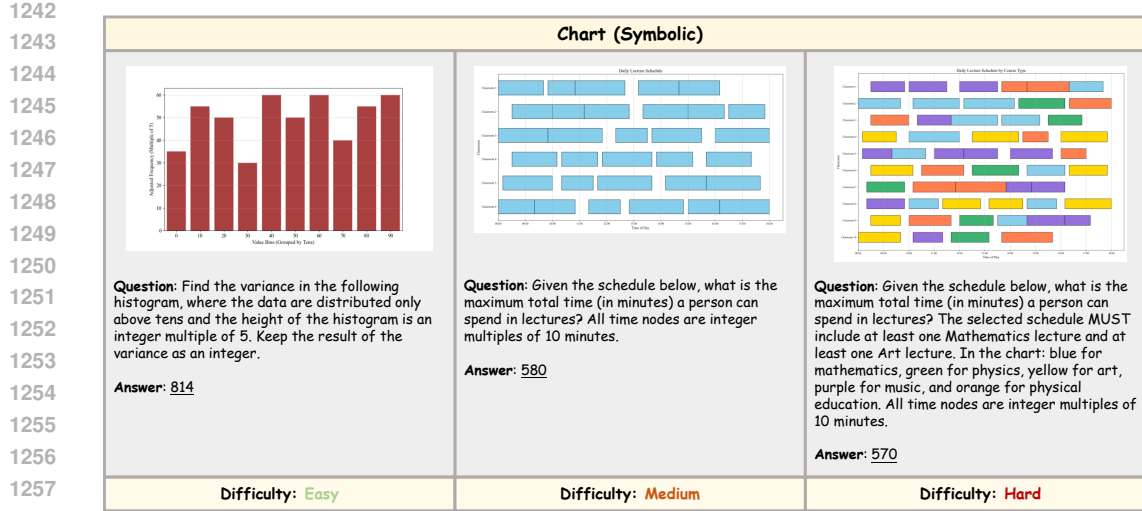


Figure 23: Data example of Chart.

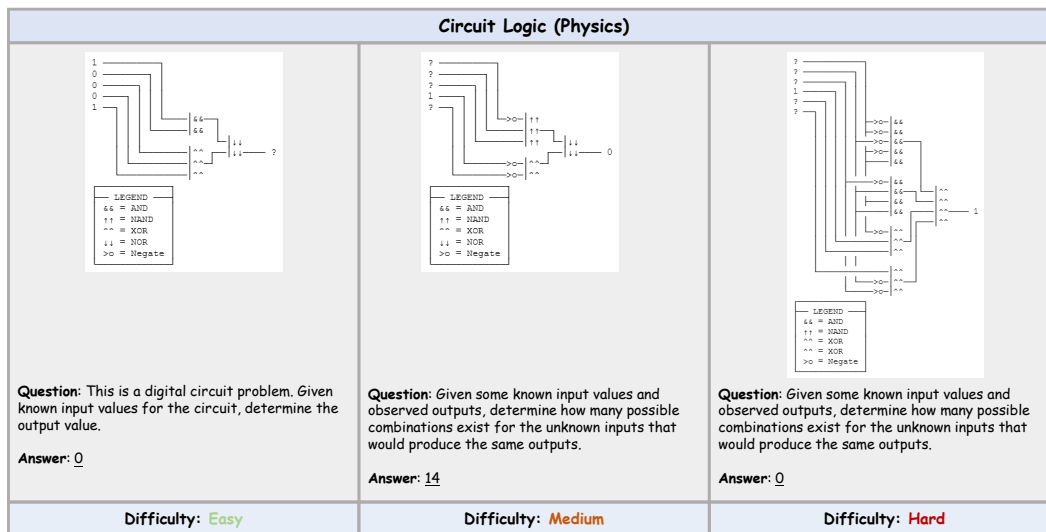


Figure 24: Data example of Circuit Logic.

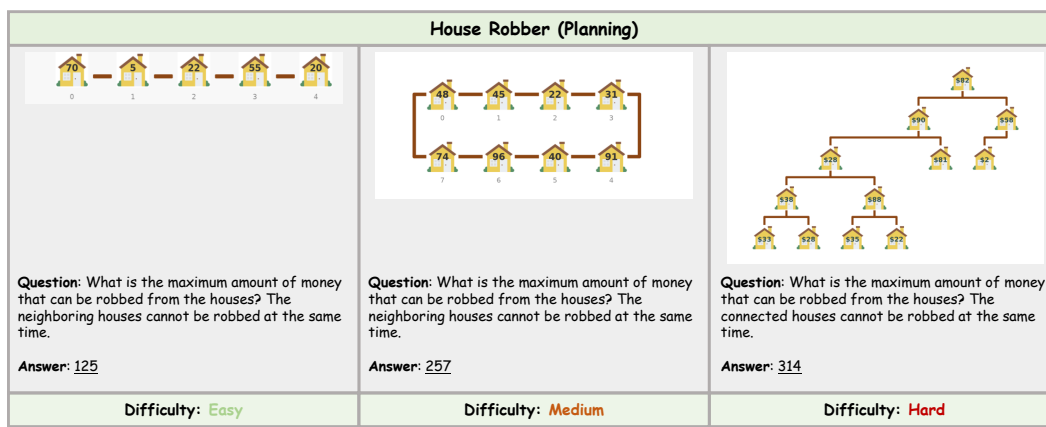


Figure 25: Data example of House Robber.

1296

1297

1298

1299

1300

1301

1302

1303

1304

1305

1306

1307

1308

1309

Interval DP (Planning)		
 <p>Question: The picture shows the balloon popping problem. You need to pop all the balloons in a certain order. The reward for a popped balloon is the product of itself and the values on the left and right balloons. If there is no balloon on the left or right, multiply the value of the balloon on the left or right by 1. You need only find the total maximum reward. Give me the number.</p> <p>Answer: <u>1</u></p>	 <p>Question: The picture shows the balloon popping problem. You need to pop all the balloons in a certain order. The reward for a popped balloon is the product of itself and the values on the left and right balloons. If there is no balloon on the left or right, multiply the value of the balloon on the left or right by 1. You need only find the total maximum reward. Give me the number.</p> <p>Answer: <u>1035613</u></p>	 <p>Question: The picture shows the balloon popping problem. You need to pop all the balloons in a certain order. The reward for popping a red balloon is the product of itself and the value on the balloons to the left and right. The reward for popping a gold balloon is doubled, and the reward for popping a black balloon becomes negative. If there is no balloon on the left or right, multiply the value by 1. You only need to find the maximum reward and keep only the final value.</p> <p>Answer: <u>1639518</u></p>
Difficulty: Easy	Difficulty: Medium	Difficulty: Hard

Figure 26: Data example of Interval DP.

1310

1311

1312

1313

1314

1315

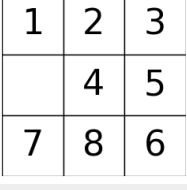
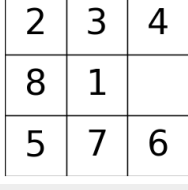
N-Puzzle (Search)		
 <p>Question: This is an 8-digit puzzle. Find the minimum number of steps to restore it.</p> <p>Answer: <u>3</u></p>	 <p>Question: This is an 8-digit puzzle. Find the minimum number of steps to restore it.</p> <p>Answer: <u>21</u></p>	 <p>Question: This is an 15-digit puzzle. Find the minimum number of steps to restore it.</p> <p>Answer: <u>17</u></p>
Difficulty: Easy	Difficulty: Medium	Difficulty: Hard

Figure 27: Data example of N-Puzzle.

1322

1323

1324

1325

1326

Tableau LP (Planning)																																																																																
<p>Problem 1: Network Parameters</p> <table border="1"> <thead> <tr> <th>Route</th><th>Cost (\$)</th><th>Capacity</th></tr> </thead> <tbody> <tr> <td>F1 → H1</td><td>10</td><td>279</td></tr> <tr> <td>H1 → F2</td><td>10</td><td>251</td></tr> <tr> <td>H1 → R1</td><td>8</td><td>151</td></tr> <tr> <td>H1 → R2</td><td>8</td><td>168</td></tr> <tr> <td>F2 → R2</td><td>5</td><td>347</td></tr> </tbody> </table> <p>Parameter Value</p> <table border="1"> <tbody> <tr> <td>Supply at F1</td><td>279</td></tr> <tr> <td>Supply at F2</td><td>0</td></tr> <tr> <td>Demand at R1</td><td>279</td></tr> <tr> <td>Demand at R2</td><td>211</td></tr> </tbody> </table> <p>Question: Given the supply, demand, and route table for this logistics problem, what is the minimum total cost? Please provide the answer as an integer.</p> <p>Answer: <u>5126</u></p>	Route	Cost (\$)	Capacity	F1 → H1	10	279	H1 → F2	10	251	H1 → R1	8	151	H1 → R2	8	168	F2 → R2	5	347	Supply at F1	279	Supply at F2	0	Demand at R1	279	Demand at R2	211	<p>Problem 1: Network Parameters</p> <table border="1"> <thead> <tr> <th>Route</th><th>Cost (\$)</th><th>Capacity</th></tr> </thead> <tbody> <tr> <td>F1 → H1</td><td>10</td><td>220</td></tr> <tr> <td>H1 → F2</td><td>10</td><td>220</td></tr> <tr> <td>H1 → R1</td><td>8</td><td>220</td></tr> <tr> <td>H1 → R2</td><td>8</td><td>220</td></tr> <tr> <td>F2 → R2</td><td>5</td><td>220</td></tr> </tbody> </table> <p>Parameter Value</p> <table border="1"> <tbody> <tr> <td>Supply at F1</td><td>321</td></tr> <tr> <td>Supply at F2</td><td>0</td></tr> <tr> <td>Demand at R1</td><td>100</td></tr> <tr> <td>Demand at R2</td><td>220</td></tr> </tbody> </table> <p>Question: Given the supply, demand, and route table for this logistics problem, what is the minimum total cost? Please provide the answer as an integer.</p> <p>Answer: <u>8085</u></p>	Route	Cost (\$)	Capacity	F1 → H1	10	220	H1 → F2	10	220	H1 → R1	8	220	H1 → R2	8	220	F2 → R2	5	220	Supply at F1	321	Supply at F2	0	Demand at R1	100	Demand at R2	220	<p>Problem 1: Network Parameters</p> <table border="1"> <thead> <tr> <th>Route</th><th>Cost (\$)</th><th>Capacity</th></tr> </thead> <tbody> <tr> <td>F1 → H1</td><td>10</td><td>264</td></tr> <tr> <td>H1 → F2</td><td>10</td><td>264</td></tr> <tr> <td>H1 → R1</td><td>8</td><td>264</td></tr> <tr> <td>H1 → R2</td><td>8</td><td>264</td></tr> <tr> <td>F2 → R2</td><td>5</td><td>264</td></tr> </tbody> </table> <p>Parameter Value</p> <table border="1"> <tbody> <tr> <td>Supply at F1</td><td>324</td></tr> <tr> <td>Supply at F2</td><td>0</td></tr> <tr> <td>Demand at R1</td><td>100</td></tr> <tr> <td>Demand at R2</td><td>264</td></tr> </tbody> </table> <p>Question: Given the supply, demand, and route table for this logistics problem, what is the minimum total cost? Please provide the answer as an integer.</p> <p>Answer: <u>6309</u></p>	Route	Cost (\$)	Capacity	F1 → H1	10	264	H1 → F2	10	264	H1 → R1	8	264	H1 → R2	8	264	F2 → R2	5	264	Supply at F1	324	Supply at F2	0	Demand at R1	100	Demand at R2	264
Route	Cost (\$)	Capacity																																																																														
F1 → H1	10	279																																																																														
H1 → F2	10	251																																																																														
H1 → R1	8	151																																																																														
H1 → R2	8	168																																																																														
F2 → R2	5	347																																																																														
Supply at F1	279																																																																															
Supply at F2	0																																																																															
Demand at R1	279																																																																															
Demand at R2	211																																																																															
Route	Cost (\$)	Capacity																																																																														
F1 → H1	10	220																																																																														
H1 → F2	10	220																																																																														
H1 → R1	8	220																																																																														
H1 → R2	8	220																																																																														
F2 → R2	5	220																																																																														
Supply at F1	321																																																																															
Supply at F2	0																																																																															
Demand at R1	100																																																																															
Demand at R2	220																																																																															
Route	Cost (\$)	Capacity																																																																														
F1 → H1	10	264																																																																														
H1 → F2	10	264																																																																														
H1 → R1	8	264																																																																														
H1 → R2	8	264																																																																														
F2 → R2	5	264																																																																														
Supply at F1	324																																																																															
Supply at F2	0																																																																															
Demand at R1	100																																																																															
Demand at R2	264																																																																															
Difficulty: Easy	Difficulty: Medium	Difficulty: Hard																																																																														

Figure 28: Data example of Tableau LP.

1348

1349

Area Measurement (Geometry)		
<p>Question: Find the area of the following quadrilateral, where all points are on integers. The result is rounded to 1 decimal place.</p> <p>Answer: <u>4.0</u></p>	<p>Question: Find the area of the following quadrilateral, where all points are on integers. The result is rounded to 1 decimal place.</p> <p>Answer: <u>4.0</u></p>	<p>Question: Find the area of the quadrilateral in the figure, where the side length of the square border is 10 and the vertices of the quadrilateral are all on points that are integer multiples of 0.5. The result is rounded to one decimal place.</p> <p>Answer: <u>5.6</u></p>
Difficulty: Easy	Difficulty: Medium	Difficulty: Hard

Figure 29: Data example of Area Measurement.

Ricochet Ball (Physics)		
<p>Question: How many ricochets will a ball launched from (1, 0, 1, 0) at 30° need to hit the target at (9, 9, 0, 0)? The ball reflects perfectly off the arena walls and mirror-obstacles.</p> <p>Answer: <u>6</u></p>	<p>Question: How many ricochets will a ball launched from (1, 0, 1, 0) at 15° need to hit the target at (9, 9, 0, 0)? The ball reflects perfectly off the arena walls and mirror-obstacles.</p> <p>Answer: <u>5</u></p>	<p>Question: How many ricochets will a ball launched from (1, 0, 1, 0) at 20° need to hit the target at (11, 9, 0, 0)? The ball reflects perfectly off the arena walls and mirror-obstacles.</p> <p>Answer: <u>8</u></p>
Difficulty: Easy	Difficulty: Medium	Difficulty: Hard

Figure 30: Data example of Ricochet Ball.

Bubble Sort (Search)		
<p>Question: The figure describes the ball exchange problem. The white ball can exchange positions with the adjacent colored balls in the 4-neighborhood. The target state is that all balls are arranged in the order of red, blue, green, and yellow from the upper left corner in the order of rows first and columns. How many exchanges are needed?</p> <p>Answer: <u>3</u></p>	<p>Question: The figure describes the ball exchange problem. The white ball can exchange positions with the adjacent colored balls in the 4-neighborhood. The target state is that all balls are arranged in the order of red, blue, green, and yellow from the upper left corner in the order of rows first and columns. How many exchanges are needed?</p> <p>Answer: <u>12</u></p>	<p>Question: The figure describes the ball exchange problem. The white ball can exchange positions with the adjacent colored balls in the 4-neighborhood. The target state is that all balls are arranged in the order of red, blue, green, yellow and purple from the upper left corner in the order of rows first and columns. How many exchanges are needed?</p> <p>Answer: <u>12</u></p>
Difficulty: Easy	Difficulty: Medium	Difficulty: Hard

Figure 31: Data example of Bubble Sort.

Bounding Box (Location)		
<p>Question: Calculate the minimum enclosing rectangle area of the following rectangle, where the sides of the enclosing rectangle must be parallel to the grid.</p> <p>Answer: <u>36</u></p>	<p>Question: Calculate the area of the circumscribed rectangle of each polygon according to its color, and then find the sum of the areas of these circumscribed rectangle. The final result only retains the sum of the areas and retains the integer.</p> <p>Answer: <u>442</u></p>	<p>Question: Calculate the area of the minimum circumscribed circle of all polygons in the graph, and keep the result as an integer.</p> <p>Answer: <u>770</u></p>
Difficulty: Easy	Difficulty: Medium	Difficulty: Hard

Figure 32: Data example of Bounding Box.

Path Counting (Computation)		
<p>Question: The green dot in the picture is the starting point, and the blue dot is the end point. Each move can only go one square to the right or down. How many different simple paths are there?</p> <p>Answer: <u>11</u></p>	<p>Question: The green dot in the picture is the starting point, and the blue dot is the end point. Each move can only go one square to the right or down. How many different simple paths are there?</p> <p>Answer: <u>232</u></p>	<p>Question: In this diagram, the green dot is the starting point and the blue dot is the destination. How many different simple paths are there?</p> <p>Answer: <u>25960704</u></p>
Difficulty: Easy	Difficulty: Medium	Difficulty: Hard

Figure 33: Data example of Path Counting.

N-Queens (Search)		
<p>Question: It is required to place a number of queens so that there is a queen in each row and column. Find the number of different placements of queens that satisfy the constraint that queens cannot attack each other.</p> <p>Answer: <u>1</u></p>	<p>Question: It is required to place a number of queens so that there is a queen in each row and column. Find the number of different placements of queens that satisfy the constraint that queens cannot attack each other. At the same time, the newly placed queen cannot be eaten by the existing knight, but there is no need to consider whether the knight will be attacked by the queen.</p> <p>Answer: <u>5</u></p>	<p>Question: The goal is to place a certain number of queens so that there is one queen in each row and column. Queens cannot attack each other, and newly placed queens cannot be captured by existing knights, but there is no need to consider whether knights can be attacked by queens. Each square on the board has a specific color, representing the cost of placing a new queen on that square. The goal is to minimize this cost while meeting these requirements.</p> <p>Answer: <u>170</u></p>
Difficulty: Easy	Difficulty: Medium	Difficulty: Hard

Figure 34: Data example of N-Queens.

1458 **D EVALUATION DETAILS**
14591460 We provide the prompts for both direct CoT reasoning and multi-turn TVP reasoning, as illustrated
1461 in Figure 35 and Figure 36.
14621463 **Prompt for Direct CoT**
14641465 **System Prompt:**1466 You FIRST think about the reasoning process as an internal monologue and then provide the final answer. The
1467 reasoning process MUST BE enclosed within <think> </think> tags. The final answer MUST BE put in
1468 \\boxed{ }. Please note that if the answer requires a numerical value, please keep only the number without
1469 punctuation, units, formulas or explanations. Don't run code in your own environment.
14701471 Figure 35: Prompt for direct CoT reasoning.
14721473 **Prompt for Multi-turn TVP**
14741475 **System Prompt:**1476 You are a visual reasoning assistant that MUST write executable Python code to solve problems. You can iterate
1477 through multiple rounds to refine your solution (maximum {N} code executions).1478 **IMPORTANT CODE FORMATTING RULES:**

- You MUST wrap your code EXACTLY with <code> and </code> tags
- Do NOT use backticks (`), triple-backticks (```), or any other delimiters
- Inside <code>...</code> put only valid Python code
- Do NOT HTML-escape characters (use <, >, &, not <, >, &)

1479 **HELPER FUNCTIONS:**

```

1 import os
2 import re
3 import typing
4 def find_original_image_name(work_dir: str = '.') -> typing.Optional[str]:
5     '''Find the original image filename, excluding processed versions'''
6     for f in sorted(os.listdir(work_dir)):
7         if not f.lower().endswith('.png'): continue
8         if f.startswith('crop_'): continue
9         if re.search(r'_m(?:\d+)?\.png$', f): continue
10        return f
11    return None
12 def processed_image_name(original_image: str) -> str:
13     '''Return processed image filename for current iteration'''
14     base, ext = os.path.splitext(original_image)
15     return f'{base}_m{iteration}{ext}'

```

1480 **CODE REQUIREMENTS:**

- Use `find_original_image_name()` to locate the input image
- Save your processed image using `processed_image_name()` (will be *_m{iteration}.png)
- Use only relative paths and work within the current directory
- Do not access network or write outside the current folder

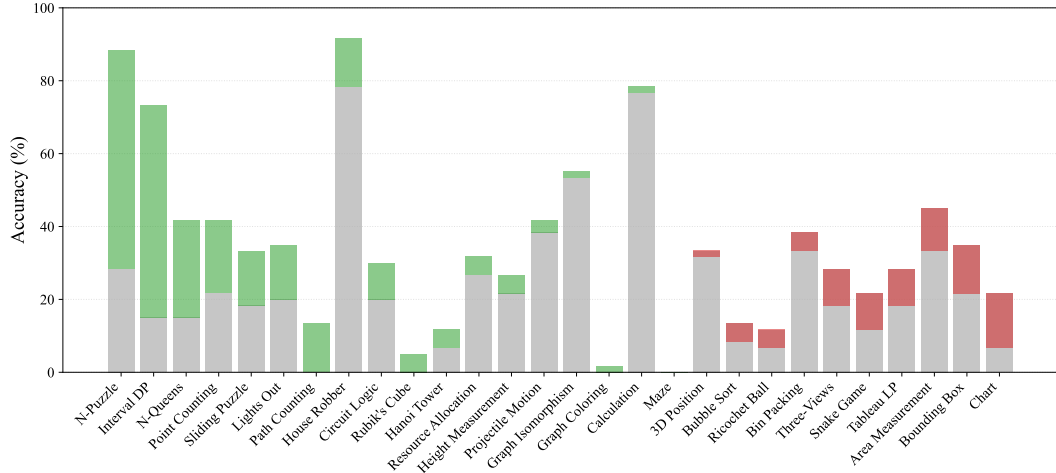
1481 **If iteration == 1:**1482 This is your FIRST iteration. Analyze the image and question carefully, then write Python code to solve it. Focus
1483 on understanding the problem and implementing a basic solution.1484 **Else:**1485 This is iteration {iteration}/{N}. You can see your previous attempts and their results in the conversation
1486 history. Analyze what went wrong in previous iterations and improve your approach. Consider the execution results
1487 and any generated images from previous attempts.1488 **Prompt for Final Answer Integration:**1489 **===== FINAL INTEGRATION =====**1490 Based on all your previous attempts, code executions, and any generated images, please provide your final answer
1491 to the original question. Original question: {question}

1492 Format your final answer using \\boxed{answer} notation.

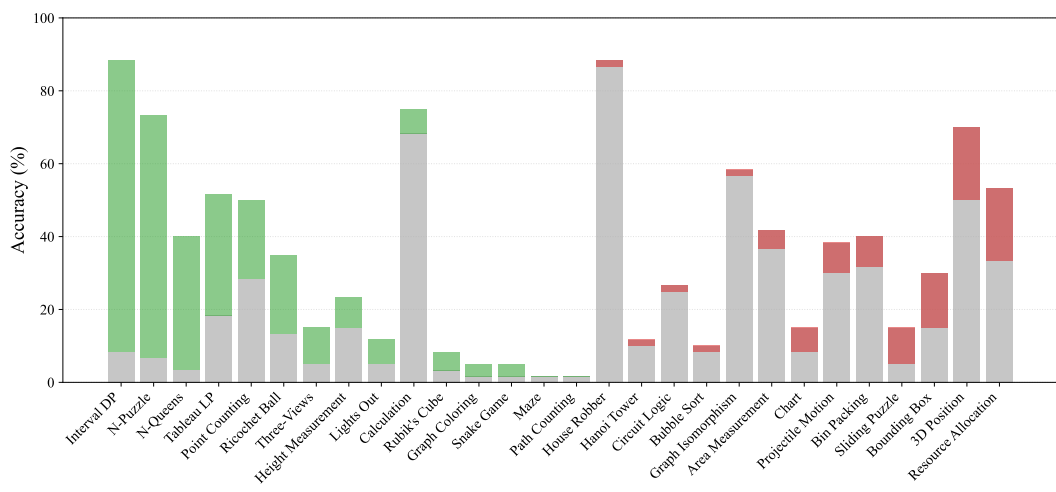
1511 Figure 36: Prompt for multi-turn TVP reasoning.

1512 E ADDITIONAL EXPERIMENTAL RESULTS

1514 As a human reference, we randomly sampled 168 instances from the benchmark and invited three
 1515 participants to solve these tasks. All participants were PhD students with strong programming back-
 1516 grounds. On average, each task required approximately 8 minutes to complete. During the process,
 1517 participants were allowed to write code and make use of search engines to access external resources
 1518 and tools when necessary.



1535 Figure 37: Performance comparison of Claude-Sonnet-4 on different tasks under CoT and TVP
 1536 ($T = 1$). Gray indicates the baseline performance of CoT, Green indicates improvements of TVP
 1537 over CoT, and Red indicates degradations of TVP over CoT.



1556 Figure 38: Performance comparison of GPT-4.1 on different tasks under CoT and TVP ($T = 5$).
 1557 Gray indicates the baseline performance of CoT, Green indicates improvements of TVP over CoT,
 1558 and Red indicates degradations of TVP over CoT.

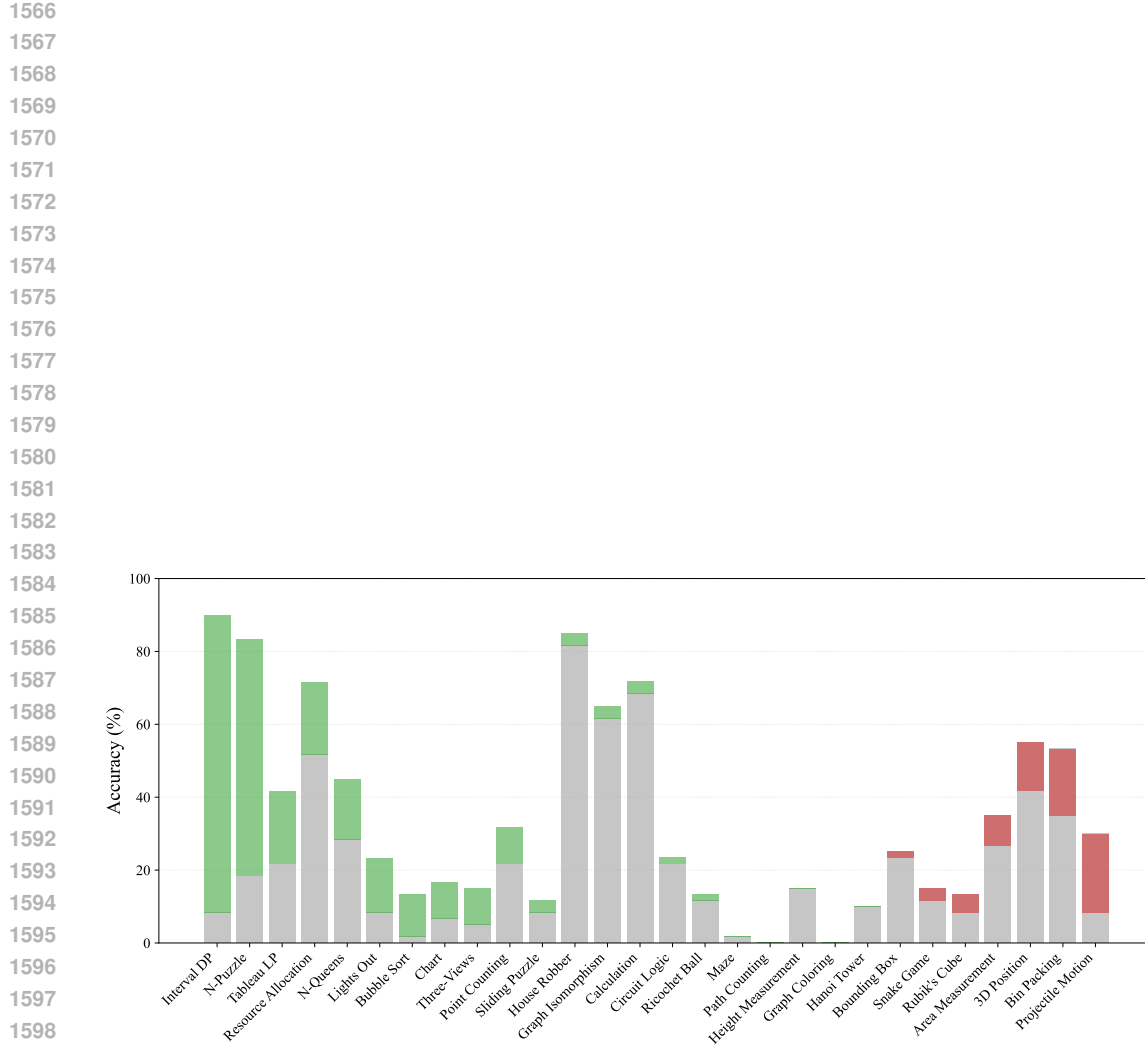


Figure 39: Performance comparison of GPT-4.1-mini on different tasks under CoT and TVP ($T = 5$). Gray indicates the baseline performance of CoT, Green indicates improvements of TVP over CoT, and Red indicates degradations of TVP over CoT.

1603
1604
1605
1606
1607
1608
1609
1610
1611
1612
1613
1614
1615
1616
1617
1618
1619

1620 **F ERROR ANALYSIS**
16211622 To better understand the limitations of TVP, we classify incorrect predictions into six categories:
1623

- 1624 • **Problem Misinterpretation.** The model misunderstands the problem requirements or constraints, leading it to pursue an incorrect solution approach.
- 1625 • **Program Execution Error.** The generated code contains syntax, logical, or runtime errors that prevent successful execution.
- 1626 • **Visual Perception Error.** The model fails to accurately extract relevant information from visual inputs, such as misrecognizing digits, shapes, or object positions.
- 1627 • **Algorithmic Modeling Error.** The model adopts an inappropriate algorithm, data structure, or fails to encode the relationships and constraints necessary for solving the problem.
- 1628 • **Program Inefficiency.** Although the solution logic is correct, the implementation is computationally inefficient and cannot handle the input within reasonable time limits.
- 1629 • **Output Formatting Issue.** The model produces outputs in an incorrect format (e.g., explanatory text instead of a numeric answer).

Problem Misinterpretation

Question: Find the variance in the following histogram, where the data are distributed only above tens and the height of the histogram is an integer multiple of 5. Keep the result of the variance as an integer.

Answer: 825

GPT-4.1 TVP (T=1)

Iteration: 1

```

1 import cv2
2 import numpy as np
3 import os
4 ...
5 heights = [55, 45, 40, 55, 50, 60, 45, 40, 50, 50]
6 bins = [5, 15, 25, 35, 45, 55, 65, 75, 85, 95]
7 filtered_bins = []
8 filtered_heights = []
9     for midpoint, freq in zip(bins, heights):
10         if midpoint > 10:
11             filtered_bins.append(midpoint)
12 ...
13 # Save the result
14 out_filename = image_filename[:-4] + '_m.png'
15 cv2.imwrite(out_filename, out_img)

```

Code Interpreter
output: "

Final Answer: \boxed{645}.

Error Cause

In the above example, while the model correctly extracted the height of each bar in the bar chart, as shown in its output, it failed to understand the meaning of the x-axis. It incorrectly interpreted the x-axis as representing the values [5, 15, 25, 35, 45, 55, 65, 75, 85, 95], misinterpreting the question's statement "where the data are distributed only above tens" as only considering data values greater than 10, thus resulting in an incorrect answer.

1670 Figure 40: Problem Misinterpretation.
1671
1672
1673

1674
1675
1676
1677
1678
1679
1680
1681
1682
1683
1684
1685
1686
1687
1688
1689
1690
1691
1692

1693
1694
1695
1696
1697
1698
1699
1700
1701
1702
1703
1704
1705
1706

1707
1708
1709
1710

1710

1715
1716
1717
1718
1719
1720
1721
1722
1723
1724
1725
1726
1727

Program Execution Error

Question: This is an 8-digit puzzle. Find the minimum number of steps to restore it.

Answer: 5

1	2	3
4	6	8
7		5

GPT-4.1-mini TVP (T=1)

Iteration: 1

```
1 import cv2
2 import numpy as np
3 from collections import deque
4 ...
5 def neighbors(state):
6     idx = state.index(0)
7     r, c = divmod(idx, 3)
8     res = []
9     for dr, dc in [(-1,0),(1,0),(0,-1),(0,1)]:
10         nr, nc = r + dr, c + dc
11         ...
12 # Save the result image
13 cv2.putText(output_img, text, (10, h-10), cv2.FONT_HERSHEY_SIMPLEX, 1,
14 (0,0,255), 2)
15 cv2.imwrite(out_filename, output_img)
```

Code Interpreter

```
error: Traceback (most recent call last):\n... line 154, in <module>\n    grid[row_i][col_i] = digit\n    ~~~~^~~~~~\nIndexError: list index out of range.\n
```

Error Cause

In the initial answer to this question, an array index out-of-bounds error caused the program to crash. In the subsequent summary answer, the model claimed that it had obtained the solution using the BFS algorithm, resulting in 6 steps (presumably based on its own reasoning), whereas the correct answer is 5 steps.

Figure 41: Program Execution Error.

1728

1729

1730

1731

1732

1733

1734

1735

1736

1737

1738

1739

1740

1741

1742

1743

1744

1745

1746

1747

1748

1749

1750

1751

1752

1753

1754

1755

1756

1757

1758

1759

1760

1761

1762

1763

1764

1765

1766

1767

1768

1769

1770

1771

1772

1773

1774

1775

1776

1777

1778

1779

1780

1781

Visual Perception Error

Question: Game Rule: Clicking a light toggles itself and its diagonal (upper-left, upper-right, lower-left, lower-right) lights. What is the minimum number of clicks required to turn off all the lights?

Answer: 10

Iteration:1
The problem describes a "lights out" type puzzle where clicking a light toggles its state and the state of its four diagonal neighbors...

```

1 import cv2
2 import numpy as np
3 import os
4 ...
5 for r_click in range(num_rows):
6     for c_click in range(num_cols):
7         k_click = rc_to_idx(r_click, c_click)
8         A[rc_to_idx(r_click, c_click), k_click] = 1
9         if r_click - 1 >= 0 and c_click - 1 >= 0:
10             A[rc_to_idx(r_click - 1, c_click - 1), k_click] = 1
11         ...
12 # Save the result image
13 output_filename = os.path.splitext(image_filename)[0] + '_m.png'
14 cv2.imwrite(output_filename, result_img)
15 print(f"Solution image saved as {output_filename}")

```

Code Interpreter
output: Detected grid size: 5 rows x 10 columns\nInitial state grid:\n[[0 1 0 0 1 0 0 1 0 0]]...Solution is unique.\nMinimum number of clicks required: 31.

Final Answer: The minimum number of clicks required to turn off all the lights is 31.

Error Cause

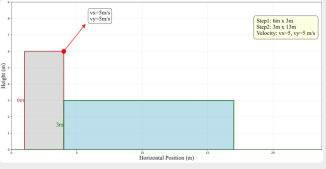
Based on the description, it seems the model understood the game rules, but differed from standard approaches to solving similar puzzle problems. During the code execution, it generated an incorrect matrix representation of the current state, leading to an incorrect solution. In the final step of summarizing and organizing the answer, the model failed to detect any anomalies in the output image, ultimately resulting in the error.

Figure 42: Visual Perception Error.

1782
1783
1784
1785
1786
1787
1788
1789
1790

1791 **Algorithmic Modeling Error**

1792

1793 

1794 **Question:** Find the horizontal coordinate of the first time the ball hits the ground. The result is rounded down to the nearest integer. Note that there is no energy loss in the event of a collision.

1795 **Answer:** 21

1796

1797

1798

1799 **Claude-Sonnet-4 TVP (T=1)**

1800 Looking at this physics problem, I need to:
1. Identify the platform heights and ball's initial position
2. ...

1801

```
1802 1 import os
1803 2 import numpy as np
1804 3 import matplotlib.pyplot as plt
1805 4 ...
1806 5 def simulate_trajectory():
1807 6     x, y = x0, y0
1808 7     vx_curr, vy_curr = vx, vy
1809 8     trajectory_x = [x]
1810 9     trajectory_y = [y]
1811 10    while t < max_time:
1812 11        x_new = x + vx_curr * dt
1813 12        ...
1814 13        plt.savefig(image_filename.replace('.png', '_m.png'), dpi=150,
1815 14        bbox_inches='tight')
1816 14    print(f"The horizontal coordinate of the first time the ball hits the ground
1817 15    is: {result}")
```

1818 **Code Interpreter**
output: The horizontal coordinate of the first time the ball hits the ground is: 20

1819

1820

1821 **Find Answer:** Looking at the physics problem, I need to simulate the ball's trajectory with elastic collisions...Finally hits the
1822 ground at x = 20

1823

1824

1825

1826

1827

1828

1829

1830

1831

1832

1833

1834

1835

Error Cause

This answer contains a clear algorithmic error. While the model correctly understood the question and extracted the relevant information, it incorrectly limited the horizontal movement of the ball to a maximum of 20 units during the simulation, whereas the correct answer was 21, which exceeded this maximum limit. The model failed to identify this flaw when summarizing and finalizing its answer.

Figure 43: Algorithmic Modeling Error.

1836
1837
1838
1839
1840
1841
1842
1843

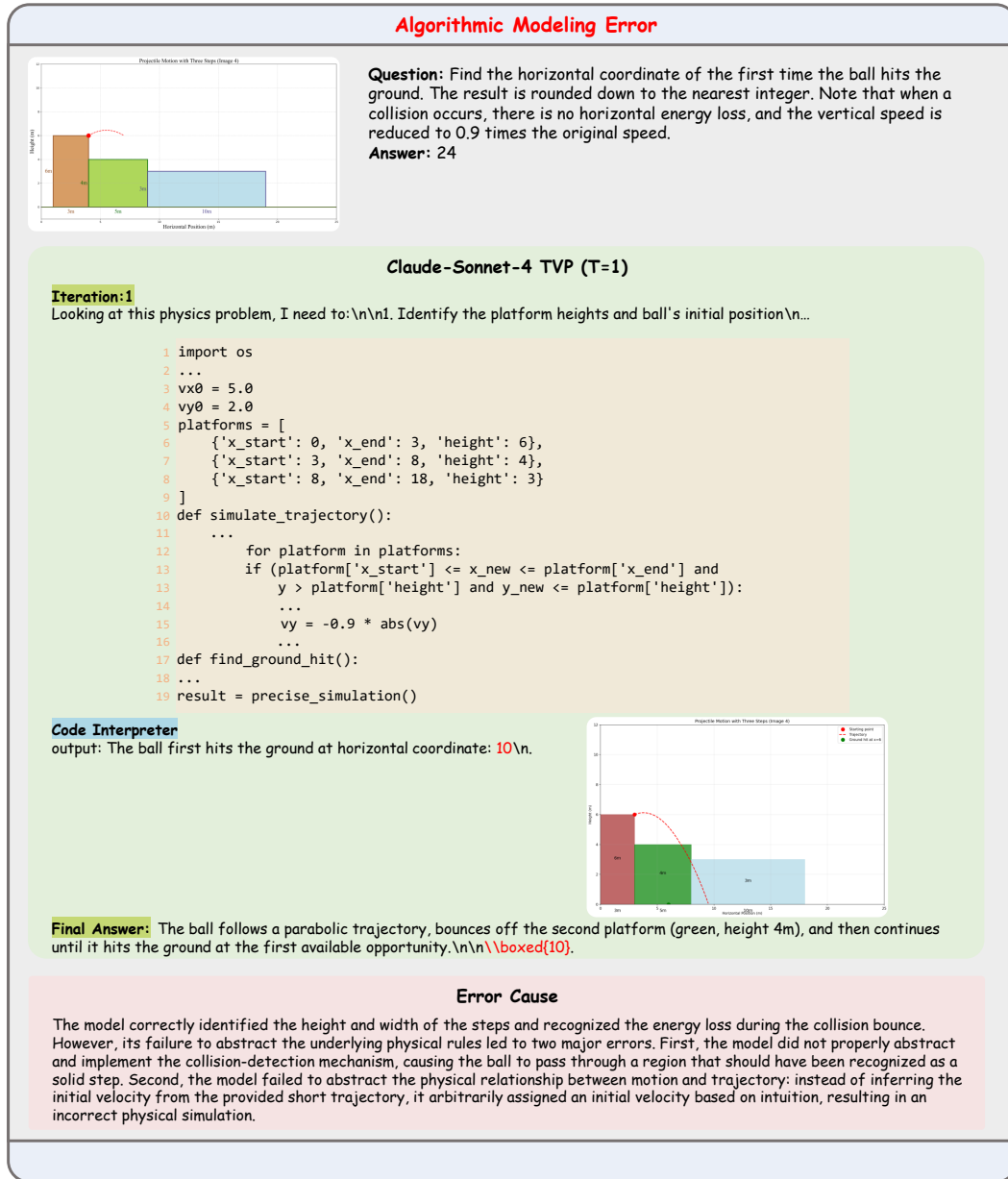


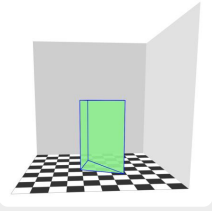
Figure 44: Algorithmic Modeling Error.

1882
1883
1884
1885
1886
1887
1888
1889

1890
1891
1892
1893
1894
1895
1896
1897
1898
1899
1900
1901
1902
1903
1904
1905
1906
1907
1908
1909
1910
1911
1912
1913
1914
1915
1916
1917
1918
1919
1920
1921
1922
1923
1924
1925
1926
1927
1928
1929
1930
1931
1932
1933
1934
1935
1936
1937
1938
1939
1940
1941
1942
1943

Algorithmic Modeling Error

Question: Estimate the volume of the 3D prism shown in the image. The result should be rounded to one decimal place. The side length of each grid on the chessboard is 0.5.
Answer: 2.3



Claude-Sonnet-4 TVP (T=1)

Iteration:1
 Looking at this physics problem, I need to:
 1. Identify the platform heights and ball's initial position
 2. ...
 3. chessboard_size = (7, 7) # Internal corners
 4. found, corners = cv2.findChessboardCorners(gray, chessboard_size, None)
 5. ...
 6. if found:
 7. criteria = (cv2.TERM_CRITERIA_EPS + cv2.TERM_CRITERIA_MAX_ITER, 30, 0.001)
 8. corners = cv2.cornerSubPix(gray, corners, (11, 11), (-1, -1), criteria)
 9. ...
 10. if contours:
 11. largest_contour = max(contours, key=cv2.contourArea)
 12. x, y, w, h = cv2.boundingRect(largest_contour)
 13. epsilon = 0.02 * cv2.arcLength(largest_contour, True)
 14. approx = cv2.approxPolyDP(largest_contour, epsilon, True)
 15. ...
 16. prism_depth = prism_width
 17. ...
 18. cv2.putText(result_img, f'Estimated Volume: {volume:.1f} cubic units',
 19. ...
 20. print(f"Visual estimated volume: {volume:.1f} cubic units")

Code Interpreter
 output: Visual estimated volume: **8.0** cubic units

Final Answer: This appears to be a rectangular prism (cube), so:

$$\text{Volume} = \text{length} \times \text{width} \times \text{height} = 2.0 \times 2.0 \times 2.0 = 8.0$$
 cubic units

Error Cause

The model attempts to locate the corner points within the checkerboard grid and then determine the positional relationships between the prism's vertices and the grid corners, as well as estimate the prism's height, to compute its volume. However, the resulting volume estimation is highly inaccurate. Ideally, the model should accurately detect all checkerboard vertices, infer the 3D-2D coordinate transformation matrix, reconstruct the prism's 3D vertex coordinates from their 2D projections, and then compute the volume. These errors reveal a clear deficiency in the model's abstraction capabilities: although it can perceive local geometric features, it fails to abstract the underlying 3D geometric principles and transformation rules required to solve the problem correctly.

Figure 45: Algorithmic Modeling Error.

1944
1945
1946
1947
1948
1949
1950
1951
1952
1953
1954
1955

1956
1957

1958
1959
1960
1961

1962
1963
1964

1965

1966

1967

1968

1969

1970

1971

1972

1973

1974

1975

1976

1977

1978

1979

1980

1981

1982

1983

1984

1985

1986

1987

1988

1989

1990

1991

1992

1993

1994

1995

1996

1997

Program Inefficiency



Question: There are some blocks in the picture. Find the smallest square area that can place all the small blocks in the area in a suitable way without overlapping. Return the length of the square side.

Answer: 4

GPT-4.1-mini TVP (T=1)

Iteration:1

```

1 from PIL import Image
2 import numpy as np
3 import os
4 ...
5 def can_place(board, block, r, c):
6     h, w = board.shape
7     bh, bw = block.shape
8     if r + bh > h or c + bw > w:
9         ...
10    def backtrack(board, blocks, idx):
11        if idx == len(blocks):
12            ...
13        blocks = extract_blocks(image)
14        answer = solve(blocks)
15        print(answer)

```

Code Interpreter
error: Code execution timed out after 60 seconds.

Final Answer: \boxed{5}.

Error Cause

In the example above, the algorithm first tries to count the total number of small squares, and then starts by trying the smallest possible square under those conditions, using a BFS method to find a feasible arrangement. However, this algorithm is too inefficient and fails to find a solution within the 60-second time limit. Therefore, the model incorrectly concluded that the minimum side length should be at least 5.

Figure 46: Program Inefficiency.

1998
1999

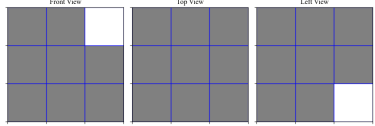
G CASE STUDY

2000
2001
2002
2003
2004
2005
2006
2007
2008
2009
2010
2011
2012
2013

We provide several case studies to analyze the performance of CoT, single-turn TVP, and multi-turn TVP. As illustrated in Figure 47, the model uses code to abstract three-dimensional views for solving the task. In contrast, CoT can only describe this process textually, lacking the ability to perform direct computation or manipulation of the visual input. As illustrated in Figure 48, TVP utilizes the model’s advanced coding capabilities to accurately model the Rubik’s Cube rotation rules. By integrating this with a search algorithm, TVP provides a precise solution, demonstrating the power of visual programming in solving complex tasks. However, for simpler problems shown in Figure 49, writing code may actually introduce errors, as the overhead of coding can outweigh the benefits of using a more direct reasoning approach. When comparing single-turn TVP with multi-turn TVP, we observe that the latter enables models to iteratively refine their outputs, effectively correcting coding mistakes through agentic interaction, as shown in Figure 50. Furthermore, Figure 51 shows cases where the model employs visualizations as an intermediate verification mechanism, ensuring that no red points are overlooked and demonstrating reflective reasoning through explicit inspection of its own outputs.

2014
2015
2016
2017
2018
2019
20202021
2022
2023
2024
2025
2026
2027
2028
2029
2030
2031

Three-Views



Question: Given a description of the three-view drawing of a solid figure, find the maximum number of small cubes that the solid figure can be composed of when the three-view constraints are met.

Answer: 21

X **GPT-4.1-mini CoT**

Direct Answer:

```
<think><The three views (front, top, left) show which small cubes are visible from each perspective...Therefore, the maximum number of small cubes is 22.</think><\\boxed{22}>
```

✓ **GPT-4.1-mini TVP (T=1)**

Iteration:1

```
<code>import os\nfrom PIL import Image\nimage_filename = None\nfor... max_cubes = 0\nfor h in range(height):\n    for w in range(width):\n        for d in range(depth):\n            if front_grid[h][w] and left_grid[h][d] and top_grid[w][d]:\n                max_cubes += 1\n...print("Maximum number of small cubes that the solid figure can be composed of:", max_cubes)\n</code>
```

Code Interpreter: output: Maximum number of small cubes that the solid figure can be composed of: 21

Final Answer: \\boxed{21}

Comparative Analysis

By comparing the two approaches, we found that in the direct reasoning (CoT) method, the model determines the total number of small cubes by sequentially analyzing whether each position can accommodate a small cube, but this method leads to errors due to double-counting. However, the approach using a single code execution (TVP) leverages three-dimensional views to model the constraints, allowing for accurate calculation of the maximum number of small cubes that can be accommodated. The advantage of using code lies in its greater accuracy when dealing with complex but repetitive (rule-based) calculations.

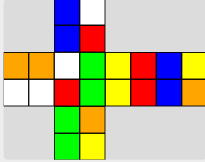
2032
2033
2034
2035
2036
2037
2038
2039
2040
2041
2042
2043
2044
2045
2046
2047
2048
2049
2050
2051

Figure 47: Case study of Tree-Views.

2052
2053
2054
2055
2056
2057
2058
2059
2060
2061
2062
2063
2064
2065

2066 **Rubik's Cube**

2067

2068 

2069 **Question:** This is the expansion diagram of a second-order Rubik's Cube. Given the initial state, you can perform 18 standard operations. Find the minimum number of steps to make the Rubik's Cube reach the restored state. The goal is to restore the cube to its original state, with green on the front face, white on the top, and yellow on the bottom, disregarding isomorphic configurations.

2070 **Answer:** 2

2071

2072 **Claude-Sonnet-4 CoT**

2073 **Direct Answer:**

2074 `<think>\I need to analyze this 2x2 Rubik's cube expansion diagram to find the minimum number of moves to solve it.\n...Based on the pattern analysis and typical solving sequences for 2x2 cubes with this level of scrambling, the minimum number of steps required is:\n\n\boxed{7}.`

2075

2076

2077

2078

2079

2080

2081

2082

2083

2084 **Claude-Sonnet-4 TVP (T=1)**

2085 **Iteration:1**

2086 I'll solve this step by step by analyzing the Rubik's cube expansion diagram.

2087 `<code>\import os\nimport numpy as np\nfrom PIL import Image\nfrom collections import deque\nimport hashlib\n...temp = [new_state['U'][0],`

2088 `new_state['U'][1]]\nnew_state['U'][0], new_state['U'][1] =`

2089 `new_state['R'][1], new_state['R'][3]]\nnew_state['R'][1],`

2090 `new_state['R'][3] = new_state['D'][3], new_state['D'][2]]\n...`

2091 `print(f"\nResult saved as {output_filename}")\n</code>`

2092 **Code Interpreter:** output: Initial cube state:\nU: ['B', 'W', 'B', 'R']\n...Solution found in 2 steps:\nL' F\nResult saved as image_20_m.png\n

2093 **Final Answer:** Looking at the code execution result,...guaranteed to be optimal (minimum number of steps).\n\n\boxed{2}

2094

2095

2096

2097

2098

2099

2100

2101

2102

2103

2104

2105

Figure 48: Case study of Rubik's Cube.

2106
 2107
 2108
 2109
 2110
 2111
 2112
 2113
 2114
 2115
 2116
 2117
 2118
 2119
 2120
 2121
 2122
 2123
 2124
 2125
 2126

Area Measurement

Question: Find the area of the following quadrilateral, where all points are on integers. The result is rounded to 1 decimal place.

Answer: 6.0

✓ **Qwen2.5-VL-32B CoT**

Direct Answer:

```
<think>To find the area of the given triangle, we can use the Shoelace Theorem...calculate the area: \n\n\n[ \n\n\text{Area} = \n\frac{1}{2} \cdot 12 = 6\n\nTherefore, the area of the triangle is: \n\n\nboxed{6.0}.
```

✗ **Qwen2.5-VL-32B TVP (T=1)**

Iteration:

```
I'll solve this step by step by analyzing the Rubik's cube expansion diagram.
<code>import os\nimport cv2\nimport numpy as np\nimport
re\n...contours, _ = cv2.findContours(image=mask, mode=cv2. RETR_LIST,
method=cv2.CHAIN_APPROX_SIMPLE)\ncentroids = []\nfor cnt in contours:
M = cv2.moments(contour)\n    if M['m00'] != 0:\n        cx =
int(M['m10'] / M['m00'])\n        cy = int(M['m01'] / M['m00'])\n
centroids.append((cy, cx))...# Save the marked image\noutput_filename =
re.sub(r'(\.).png', ' _m\\1', image_filename)\ncv2.imwrite(output_filename, cv2.cvtColor(image,
cv2.COLOR_BGR2RGB))\n</code>
```

Code Interpreter: error: ...line 36\n contours, _ = cv2.findContours\ntmask, cv2.
RETR_LIST, cv2.CHAIN_APPROX_SIMPLE)\n
^SyntaxError: unmatched ')'\n

Final Answer: None

Comparative Analysis

Comparing CoT and TVP (T=1), we can see that CoT accurately obtained the coordinates of the points directly from the image information and then used the quadrilateral area formula to calculate the area accurately. However, the code provided by TVP attempted to identify the vertices of the quadrilateral to calculate the area, but it failed to correctly locate the vertices, resulting in an error. Therefore, for models with limited coding capabilities, using code to assist in problem-solving may actually lead to lower accuracy than simply providing a direct answer.

2143
 2144
 2145
 2146
 2147
 2148
 2149
 2150
 2151
 2152
 2153
 2154
 2155
 2156
 2157
 2158
 2159

Figure 49: Case study of Area Measurement.

2160

2161

2162

2163

2164

2165

2166

2167

2168

2169

2170

2171

2172

2173

2174

2175

2176

2177

2178

2179

2180

2181

2182

2183

2184

2185

2186

2187

2188

2189

2190

2191

2192

2193

2194

2195

2196

2197

2198

2199

2200

2201

2202

2203

2204

2205

2206

2207

2208

2209

2210

2211

2212

2213

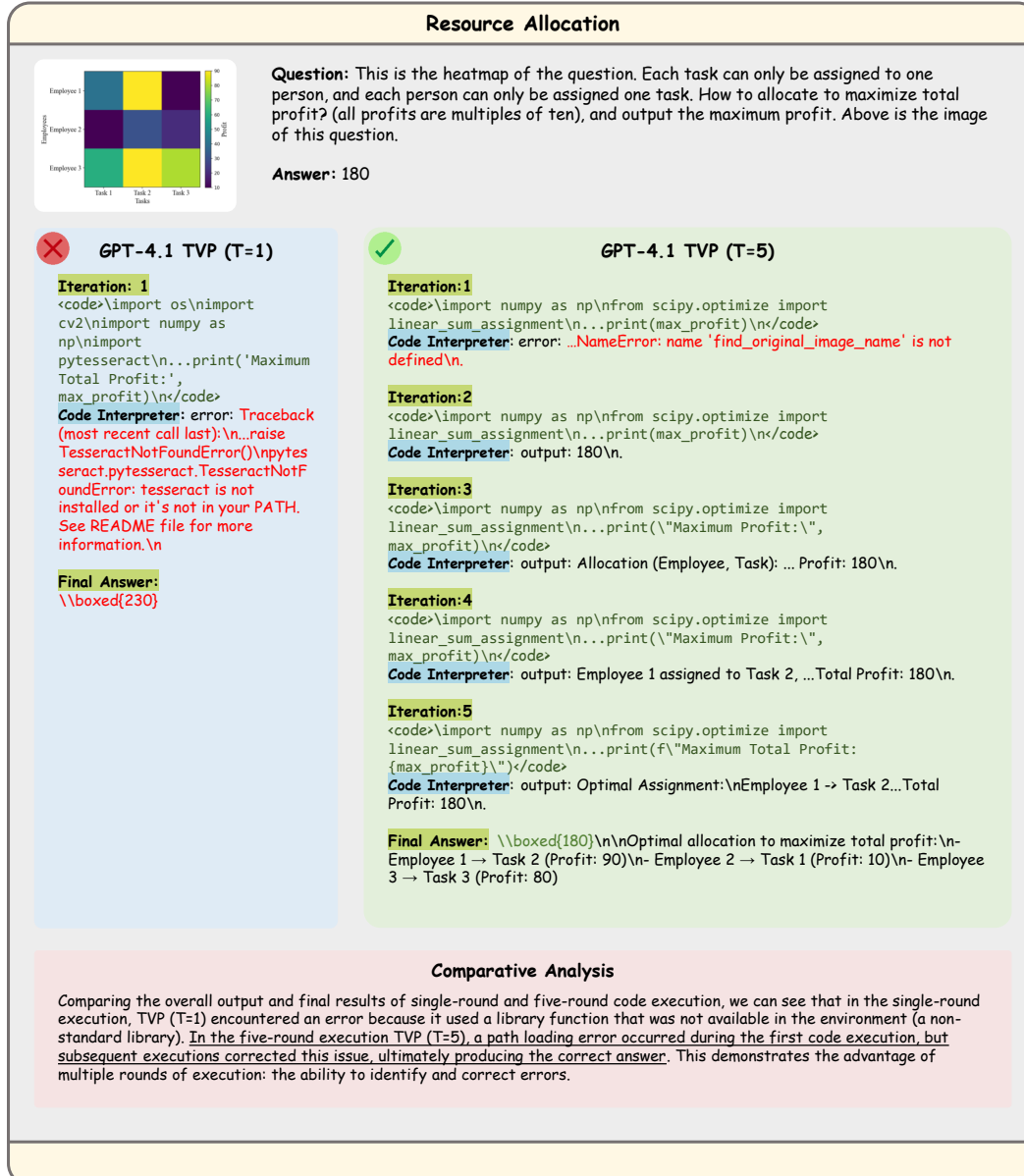


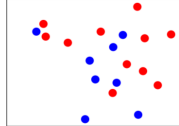
Figure 50: Case study of Area Measurement.

2214
 2215
 2216
 2217
 2218
 2219
 2220
 2221
 2222
 2223
 2224
 2225
 2226
 2227
 2228
 2229
 2230
 2231

Point Counting

Question: What is the number of red dots?

Answer: 11



Gemini-2.5-Flash TVP (T=1)

Iteration: 1
`<code>\import os\nimport cv2\nimport numpy as np\n\n...cv2.imwrite(output_filename, original_image)\n</code>`
Code Interpreter: output: Could not find a suitable red dot to create a template. Falling back to direct contour counting.\nNumber of red dots (contour fallback): 0\n**Final output:** `<code>\import os\nimport cv2\nimport numpy as np\n\n...cv2.imwrite(output_filename, original_image)\n</code>`

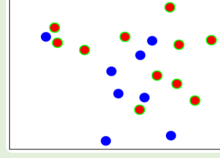
Final Answer:
 None



Gemini-2.5-Flash TVP (T=3)

Iteration:1
`<code>\import cv2\nimport numpy as np\n\n...output_image_path = processed_image_name(image_path)\nncv2.imwrite(output_image_path, output_image)\n</code>`
Code Interpreter: error: ...NameError: name 'find_original_image_name' is not defined\n.

Iteration:2
 The previous attempt failed because...The image processing logic for counting red dots.
`<code>\ \import cv2\nimport numpy as np\n\n...output_image_path = processed_image_name(image_path)\nncv2.imwrite(output_image_path, output_image)\n</code>`
Code Interpreter: output: The number of red dots is: 11\n.



Iteration:3
 The number of red dots is: 11\n

Final Answer:
 The number of red dots is: \boxed{11}

Comparative Analysis

Comparing the overall output and final results of single-round and three-round code execution, we can see that in the single-round execution, TVP (T=1) encountered an error because the algorithm failed to detect any red points because of an incorrect threshold setting. In the three-round execution TVP (T=3), a path loading error occurred during the first code execution, but subsequent executions corrected this issue, ultimately producing the correct answer. Next, after receiving the corresponding text and image results, it confirmed that all the red dots had been found, thus pre-determining the answer.

2257
 2258
 2259
 2260
 2261
 2262
 2263
 2264
 2265
 2266
 2267

Figure 51: Case study of Point Counting.

2268

2269

2270

2271

2272

2273

2274

2275

2276

2277

2278

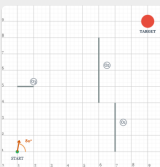
2279

2280

2281

2282

2283



Question: How many ricochets will a ball launched from $(1.0, 1.0)$ at 80° need to hit the target at $(9.0, 9.0)$? The ball reflects perfectly off the arena walls and mirror-obstacles.

Answer: 7

✗ Gemini-2.5-Flash TVP (T=1)

Iteration: 1
 The problem requires simulating the path of a ball launched from a starting point with a given angle...
 <code>\import math\nimport os\nimport re\nimport typing\nimport matplotlib.pyplot as plt\nimport matplotlib.patches as patches\n...def get_time_to_hit_target(current_pos, current_velocity, target_pos, target_radius):\n dx = current_pos.x - target_pos.x\n dy = current_pos.y - target_pos.y\n ... # Print the final answer\n \n</code>

Code Interpreter: output: "7\n"

Final Answer:
 10

✓ Gemini-2.5-Flash TVP (T=3)

Iteration:1
 <code>\import math\nimport os\nimport re\nimport typing\nimport matplotlib.pyplot as plt\nimport matplotlib.patches as patches\n...def get_time_to_hit_target(current_pos, current_velocity, target_pos, target_radius):\n dx = current_pos.x - target_pos.x\n dy = current_pos.y - target_pos.y\n ... # Print the final answer\n \n</code>

Code Interpreter: output: "7\n"

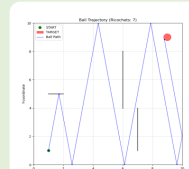
Iteration:2
 The previous iteration's code correctly calculated 7 ricochets and produced a visual path that supports this answer...

<code>\import math\nimport os\nimport re\nimport typing\nimport matplotlib.pyplot as plt\nimport matplotlib.patches as patches\n...def get_time_to_hit_wall(current_pos, current_velocity):\n dt_x = float('inf')\n dt_y = float('inf')\n ...# Print the final answer\n \n</code>

Code Interpreter: error: ...~~~~~\nNameError: name 'find_original_image_name' is not defined\n

Iteration:3
 <code>\import math\nimport os\nimport re\nimport typing\nimport matplotlib.pyplot as plt\nimport matplotlib.patches as patches\n...# Snap position to the wall\n if abs(current_pos_next.y - Y_MIN) < EPS: current_pos_next.y = Y_MIN\n if abs(current_pos_next.y - Y_MAX) < EPS: current_pos_next.y = Y_MAX\n ...# Print the final answer\n \n</code>

Code Interpreter: output: "7\n"



Final Answer: The final answer is $\boxed{7}$

Comparative Analysis

Comparing TVP (T=1) and TVP (T=3), we can see that when only one iteration of the code is used, the model fails to find a solution within a certain number of steps due to errors in its modeling of the overall layout, resulting in a return value of -1. However, with multiple iterations, although the second iteration encountered a path-related error, the first and third iterations executed correctly, and the model successfully used the code to generate a simulated path diagram, which can assist the model in making decisions.

Figure 52: Case study of Ricochet Ball.

2311

2312

2313

2314

2315

2316

2317

2318

2319

2320

2321